

THESIS

DEVELOPMENT AND THERMAL CHARACTERIZATION OF POLYDIACETYLENE  
(PDA) NANOFIBER COMPOSITES FOR SMART WOUND DRESSING APPLICATIONS

Submitted by

A K M Mashud Alam

Department of Design and Merchandising

In partial fulfillment of the requirements

For the Degree of Master of Science

Colorado State University

Fort Collins, Colorado

Summer 2016

Master's Committee:

Advisor: Yan Vivian Li

Juyeon Park

Claudia Gentry-Weeks

Copyright by A K M Mashud Alam 2016

All Rights Reserved

## ABSTRACT

### DEVELOPMENT AND THERMAL CHARACTERIZATION OF POLYDIACETYLENE (PDA) NANOFIBER COMPOSITES FOR SMART WOUND DRESSING APPLICATIONS

Conventional methods of identification of microbiological pathogens infection in wound have many challenges such as the need for specialized instruments and trained personnel, and the long detection time. There is a critical need for an innovative method that is simple, accurate, sensitive, reliable, and rapid in pathogen detection practices. Wound dressings containing PDA nanofibers could be used as a diagnostic tool for the detection of onsite bacterial infection. By early wound infection diagnosis, the smart wound dressing would allow physicians to start timely treatment which would reduce hospitalization time and patient suffering. PDAs are of great interest in the development of chromatic sensors due to their unique optical property of undergoing a chromatic transition from blue to red upon external stimuli. 10,12-Pentacosadiynoic acid (PCDA) and poly (ethylene oxide) (PEO) were used in this study to develop fiber composites via an electrospinning method at various mass ratios of PEO to PCDA, solution concentrations, and injection speeds. High mass ratios of PEO to PCDA, low polymer concentrations, and low injection speed promoted fine fibers with smooth surfaces. The colorimetric transition of the fibers was investigated by heating the fibers at temperatures ranging from 25 °C to 120 °C. A color switch from blue to red was observed when the fibers were treated at temperatures higher than 60 °C. The color transition was more sensitive in the fibers made with a low mass ratio of PEO to PCDA due to the high fraction of PDA in the fibers. The large diameter fibers also promoted the color switch due to the high reflectance area in the

fibers. All of the fibers were analyzed using Fourier transform infrared spectroscopy (FT-IR) and differential scanning calorimetry (DSC) and compared before and after the color change occurred. The colorimetric transitional mechanism is proposed to occur due to conformational changes in the PDA macromolecules.

**Keywords:** polydiacetylene; electrospun fiber; biosensor; color transformation

## ACKNOWLEDGEMENTS

- The creator of the universe, Almighty Allah, for providing me the courage and all I required for finishing up my degree requirements.
- First and foremost, Dr. Yan Vivian Li, my academic advisor and mentor, a Professor of almost limitless patience, the depths of which may never have been fully probed if she hadn't accepted me as her student.
- Dr. Juyeon Park and Dr. Claudia Gentry-Weeks, for making time in their busy schedules to serve on my committee. Their scientific advice and insightful discussions and suggestions had always been my inspiration. Special thanks to Dr. Claudia Gentry-Weeks for her on-hand training with motherly affection on working procedures with microbes.
- Dr. Nancy Miller and Dr. Jennifer Ogle for their unconditional support and trust at all times.
- Dr. Mellissa M. Reynolds, for kind permission of using her lab. Pamela J. Yapor, for all her help and support in conducting the experiments.
- Bioscience Discovery Evaluation Grant Program (BDEGP) of the state of Colorado and Agricultural Experiment Station at Colorado State University for their financial support of this work.
- My parents, brothers, sister, wife, and daughters for their prayer, inspiration and support. My special gratitude goes to my wife for supporting my dream, and accompanying me here accepting a difficult life.

## TABLE OF CONTENTS

ABSTRACT.....	ii
ACKNOWLEDGEMENTS.....	iv
LIST OF TABLES.....	vii
LIST OF FIGURES.....	ix
CHAPTER 1. INTRODUCTION.....	1
CHAPTER 2. LITERATURE REVIEW.....	4
2. Biosensors.....	4
2.1. Conjugated Polymers (CPs).....	7
2.2. Polydiacetylene (PDA).....	7
2.2.1 Self- assembled Molecular Structures.....	8
2.2.2 Colorimetric Transition.....	9
2.2.3. PDA Nanofibers.....	10
2.2.4. Electrospinning Apparatus.....	11
2.2.5. Electrospinning Parameters.....	12
2.2.6. Solution Parameters.....	12
2.2.7. Process Parameters.....	13
2.2.8. Ambient Conditions.....	14
2.3. Color Analysis.....	14
CHAPTER 3. MATERIALS AND METHODS.....	16
3.1 Materials.....	16
3.2 Methods.....	16
3.2.1 Preparation of PDA.....	16
3.2.2 PDA Fiber Composites.....	17
3.2.3 Fiber Characterization.....	17
3.2.4. Colorimetric Transition due to Temperature.....	18
CHAPTER 4. MANUSCRIPT.....	20
Study of Polydiacetylene-Poly (Ethylene Oxide) Electrospun Fibers Used as Biosensors.....	20
SYNOPSIS.....	20
1. Introduction.....	21

2. Results and Discussion .....	24
3. Materials and Methods .....	35
4. Conclusions .....	39
REFERENCES .....	43
CHAPTER 5. CONCLUSIONS .....	47
REFERENCES .....	50
APPENDICES .....	61
Appendix 1: Fiber diameter distribution of the prepared samples .....	61
Appendix 2: Reflectance values for fiber composites prepared at 2:1 PEO: PCDA.....	62
Appendix 3: Reflectance values for fiber composites prepared at 3:1 PEO: PCDA.....	68
Appendix 4: Reflectance values for fiber composites prepared at 4:1 PEO: PCDA.....	74

## LIST OF TABLES

Table 1 Electrospinning design for preparing Polyethylene oxide (PEO)-Pentacosadiynoic acid (PCDA) fibers. ....	37
Table 2. Average diameter of the electrospun PEO-PDA fibers. ....	61
Table 3. Spectral reflectance data of the fiber composite (# 1) prepared at 2:1 PEO: PCDA, 1.5 w/w % concentration, and 0.1 ml hr <sup>-1</sup> injection speed. ....	62
Table 4. Spectral reflectance data of the fiber composite (# 2) prepared at 2:1 PEO: PCDA, 1.5 w/w % concentration, and 0.2 ml hr <sup>-1</sup> injection speed. ....	63
Table 5. Spectral reflectance data of the fiber composite (# 3) prepared at 2:1 PEO: PCDA, 3.75 w/w % concentration, and 0.1 ml hr <sup>-1</sup> injection speed. ....	64
Table 6. Spectral reflectance data of the fiber composite (# 4) prepared at 2:1 PEO: PCDA, 3.75 w/w % concentration, and 0.2 ml hr <sup>-1</sup> injection speed. ....	65
Table 7. Spectral reflectance data of the fiber composite (# 5) prepared at 2:1 PEO: PCDA, 7.5 w/w % concentration, and 0.1 ml hr <sup>-1</sup> injection speed. ....	66
Table 8. Spectral reflectance data of the fiber composite (# 6) prepared at 2:1 PEO: PCDA, 7.5 w/w % concentration, and 0.2 ml hr <sup>-1</sup> injection speed. ....	67
Table 9. Spectral reflectance data of the fiber composite (# 7) prepared at 3:1 PEO: PCDA, 1.33 w/w % concentration, and 0.1 ml hr <sup>-1</sup> injection speed. ....	68
Table 10. Spectral reflectance data of the fiber composite (# 8) prepared at 3:1 PEO: PCDA, 1.33 w/w % concentration, and 0.2 ml hr <sup>-1</sup> injection speed. ....	69
Table 11. Spectral reflectance data of the fiber composite (# 9) prepared at 3:1 PEO: PCDA, 3.34 w/w % concentration, and 0.1 ml hr <sup>-1</sup> injection speed. ....	70

Table 12. Spectral reflectance data of the fiber composite (# 10) prepared at 3:1 PEO: PCDA, 3.34 w/w % concentration, and 0.2 ml hr <sup>-1</sup> injection speed.....	71
Table 13. Spectral reflectance data of the fiber composite (# 11) prepared at 3:1 PEO: PCDA, 6.67 w/w % concentration, and 0.1 ml hr <sup>-1</sup> injection speed.....	72
Table 14. Spectral reflectance data of the fiber composite (# 12) prepared at 3:1 PEO: PCDA, 6.67 w/w % concentration, and 0.2 ml hr <sup>-1</sup> injection speed.....	73
Table 15. Spectral reflectance data of the fiber composite (# 13) prepared at 4:1 PEO: PCDA, 1.25 w/w % concentration, and 0.1 ml hr <sup>-1</sup> injection speed.....	74
Table 16. Spectral reflectance data of the fiber composite (# 14) prepared at 4:1 PEO: PCDA, 1.25 w/w % concentration, and 0.2 ml hr <sup>-1</sup> injection speed.....	75
Table 17. Spectral reflectance data of the fiber composite (# 15) prepared at 4:1 PEO: PCDA, 3.13 w/w % concentration, and 0.1 ml hr <sup>-1</sup> injection speed.....	76
Table 18. Spectral reflectance data of the fiber composite (# 16) prepared at 4:1 PEO: PCDA, 3.13 w/w % concentration, and 0.2 ml hr <sup>-1</sup> injection speed.....	77
Table 19. Spectral reflectance data of the fiber composite (# 17) prepared at 4:1 PEO: PCDA, 6.25 w/w % concentration, and 0.1 ml hr <sup>-1</sup> injection speed.....	78
Table 20. Spectral reflectance data of the fiber composite (# 18) prepared at 4:1 PEO: PCDA, 6.25 w/w % concentration, and 0.2 ml hr <sup>-1</sup> injection speed.....	79

## LIST OF FIGURES

Figure 2-1 Global biosensor market forecast, 2014-2020 .....	5
Figure 2-2 The total biosensors market, showing the percent of revenues by vertical markets (world) for 2009 and 2016 .....	6
Figure 2-3 Polymerization of DA monomer .....	9
Figure 2-4 Absorption spectral and color changes of a PDA solution that take place upon stimulation.....	10
Figure 2-5 Schematic set up of a basic vertical electrospinner.....	11
Figure 2-6 Graphical representation of the CIELAB L*,a*,b* value three dimensional space ...	15
Figure 4-1 Schematic representation of the electrospinning of poly (ethylene oxide) (PEO) – Polydiacetylene (PDA) composite fibers.....	25
Figure 4-2 Fiber diameters are illustrated as a function of polymer concentration, mass ratios of PEO and PCDA, and injection speed.....	26
Figure 4-3 SEM images of PEO-PDA electrospun fibers. ....	28
Figure 4-4 (A): Reflectance spectra of the selected PEO-PDA fiber (Fiber #9) treated at selected temperatures (25 °C, 60 °C, 70 °C, 90 °C, 100 °C, and 120 °C).....	29
Figure 4-5 Normalized reflectance spectra of 18 fibers that were heated at 70 °C for 10 minutes. .....	31
Figure 4-6 Fourier transform infrared spectroscopy (FT-IR) spectra of PEO-PDA fibers and PDA polymers.....	32
Figure 4-7 Differential scanning calorimetry (DSC) plot of PEO-PDA fibers: .....	34

Figure 4-8 An illustration of color transition from blue to red in PEO-PDA fiber mat, which is due to a C-C bond rotation induced by heat treatment. .... 35

## CHAPTER 1. INTRODUCTION

The development of advanced medical textiles for wound healing, drug delivery, tissue regeneration, sensing, and diagnostics is changing the face of the medical industry and providing doctors with tools and technology to improve patient care in dramatic ways. The intersection of smart textiles and medicine presents a range of intriguing opportunities for advancing medical diagnostics, sensing, and treatment. Advanced wound care, one of the most important segments of the medical device products, has seen a slow emergence of “smart bandages”, wound dressings that have some additional degree of built-in functionality. A wound dressing that provides early visual indication of the onset of bacterial infection, would offer physicians early wound infection diagnoses, allowing for timely treatment, reduced hospitalization time and improved patient outcome (Dargaville, et al., 2013).

Wound management is extremely challenging due to the complexity of the wound itself and the healing process. Knowledge that keeping a wound moist accelerates the healing process, as reported in his milestone study on wound management by Winter in 1962, was the start of research in this discipline (Dargaville et al., 2013). Other crucial developments have been the use of anti-microbial agents (i.e. silver and iodine), hyperbaric oxygen therapy (breathing 100% oxygen at elevated pressure), skin grafts, and compression pressure therapy. Dargaville et al. (2013) pointed out that smart dressings would be the next revolution in wound care practice where sensors would be used as a diagnostic tool in the wound healing process. This smart sensor would be critical in the management of wounds highly susceptible to infection like chronic ulcers, acute wounds, burn patients etc., where a lengthy delay in treatment creates difficulty in the healing process (Dargaville et al., 2013).

Conjugated polymers (CPs) have been widely used in the development of chemosensors and biosensors because they exhibit unique electronic and optical properties induced by external stimuli. CPs are able to detect extremely small quantities of analytes due to their ability to amplify sensory signals (Lee, Povlich, & Kim, 2010). A wide variety of conjugated polymers including polyacetylenes (Gerard, Chaubey, & Malhotra, 2002), polydiacetylenes (Chae et al., 2007; Ahn & Kim, 2008; Chen, Zhou, Peng, & Yoon, 2012; Jelinek, & Ritenberg, 2013), polyphenylene (Çete & Bal, 2013), polythiophenes (Marsella & Swager, 1993; Lee, Povlich, & Kim, 2010), polyanilines, and poly(phenylene ethynylenes) (Tan, Atas, Müller, Pinto, Kleiman, & Schanze, 2004; Pun, Lee, Kim, & Kim, 2006) have been investigated for the use in chemo- and biosensor applications (Ahn & Kim, 2008).

Among these conjugated polymers, polydiacetylenes are of great interest due to many advantages in molecular structure, method of preparation, and sensing properties (Ahn & Kim, 2008; Jelinek and Ritenberg, 2013). PDA, synthesized by a photopolymerization method with 254nm UV light, shows a blue-to-red chromatic change visible to unaided eyes in response to external stimuli such as pH and temperature (Chae et al., 2007; Yoon and Kim, 2008). Since no catalysts or initiators are required in the polymerization, PDAs are highly pure in composition. Electrospinning of PDAs without another polymer is challenging because the viscosity of PDA solutions is relatively low (Yoon and Kim, 2008). When mixed with another polymer that is able to increase the viscosity of the spinning solution, PDAs can be incorporated into fiber composites via electrospinning. The other polymer serves as a supportive component in the fiber composites and hence is named the matrix polymer. Polyethylene oxide (PEO), a biocompatible flexible polymer, is used as a matrix polymer to facilitate electrospinning of PDA nanofiber embedded in PEO (Bhattarai, Edmondson, Veiseh, Matsen, & Zhang, 2005). The high surface

area to volume ratio of the nanofibers provides increased sensitivity of the sensor system as well as reduces response time due to an increased number of sites for analytic interaction or signal transduction, (Steyaert, Rahier, & De Clerck, 2015). PDA-based chemosensors built on electrospun nanofibrous matrices have been explored for the creation of highly sensitive sensors, besides pathogen detection, for hazardous chemical compounds including volatile organic compounds (Yoon, Chae, & Kim, 2007), lead ions (Wang et al., 2015), and hydrochloric acid (Jeon, Lee, Kim, & Yoon, 2012).

The objective of this research is to develop PDA nanofiber composites using an electrospinning technique and to evaluate the colorimetric transitional properties of these composites, as a function of temperature, for their potential application as a wound dressing biosensor.

## CHAPTER 2. LITERATURE REVIEW

### 2. Biosensors

Biosensors are tools for the analysis of bio-material samples to gain an understanding of bio-composition, structure and function by converting a biological response into a signal. A conventional biosensor is composed of two basic elements including a biological recognition unit and a transducer that converts a biological response into a measurable signal. Characteristic properties of a biosensor are selectivity, sensitivity, precision, and response time (Lee, Polvich, and Kim, 2010). The selectivity of the sensor defines the ability of the sensor to detect the presence of certain bio-organisms. The sensitivity of the sensor indicates the minimum change that the sensor can detect. Precision is usually characterized using the standard deviation of the measurements. Response time refers to the time required to convert a detection event into a measurable signal.

One of the conventional biosensors is the blood glucose meter that was invented by Clarke & Lyons in 1962 and commercialized by Clemens in 1971. A glucometer utilizes a test strip containing glucose oxidase that can react with glucose. A drop of blood is placed on the test strip; the strip is inserted into the glucometer. A series of chemical reactions between blood glucose and glucose oxidase produces ferrocyanide. The ferrocyanide generates an electrical signal that is converted to a corresponding digital read on the meter, indicating the amount of glucose in the blood. It is widely used by diabetic patients to self-monitor blood glucose at home (Clarke and Foster, 2012). Recently, the biosensor market is undergoing a paradigm shift towards advanced medical applications such as infectious disease monitoring, blood gas analyses, cholesterol testing, and pregnancy testing. Biosensors also attract great interest in

many non-medical applications such as industrial biology, food safety and military services. Ongoing research and innovation in biosensors has ensured its penetration into new areas such as security, military biodefense, environmental monitoring, and the process industry (Thusu, 2010). According to a new market report published by Transparency Market Research “Biosensors Market - Global Industry Analysis, Size, Share, Growth, Trends and Forecast, 2014 - 2020,” the global biosensors market was valued at USD 12.4 billion in 2013 and is expected to grow at a compounded annual growth rate (CAGR) of 8.1% to reach USD 21.64 billion in 2020. Figure 2.1 shows the global biosensor market forecast to 2020. A high growth rate is found in home health care and point of care testing. Higher precision and accuracy, shorter response time, painless diagnosis, user friendliness and cost effectiveness have triggered the rise of the market growth. Figure 2.2 illustrates the comparative market share of different segments in the market. The percent of revenues such as environmental, security and biodefense, and home diagnostics are forecasted to continue the growth trend until 2016 (Thusu, 2010).

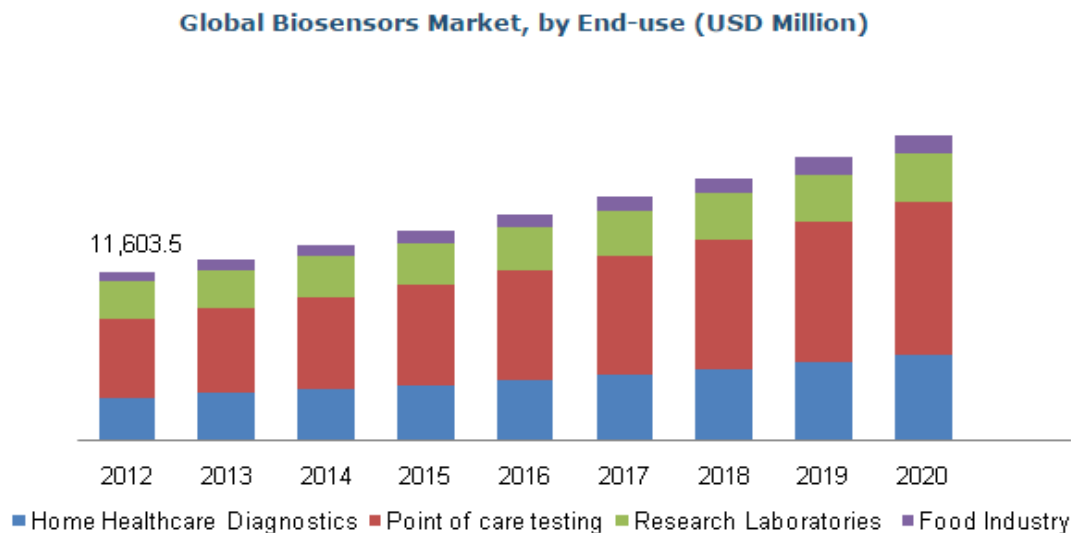


Figure 2-1 Global biosensor market forecast, 2014-2020

(Retrieved from <http://www.grandviewresearch.com/industry-analysis/biosensors-market>)

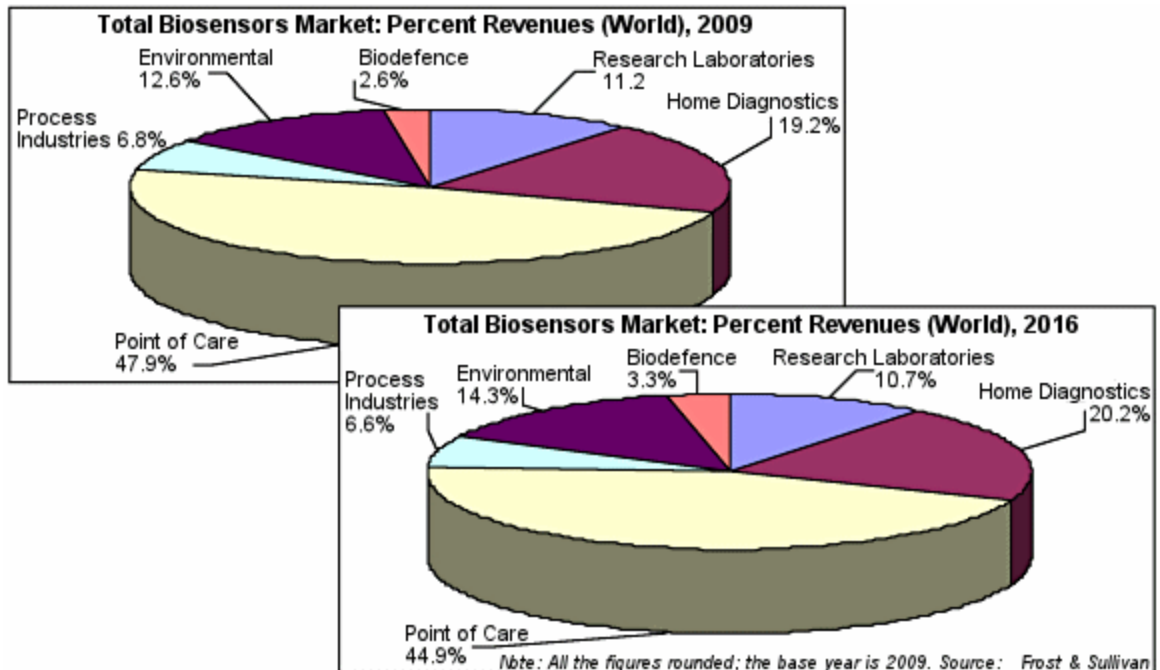


Figure 2-2 The total biosensors market, showing the percent of revenues by vertical markets (world) for 2009 and 2016 (Thus, 2010)

One promising application of advanced biosensors is to detect pathogenic bacterial infections in hygiene processes such as food preparation and wound care. Conventional approaches include a culture and colony counting method, an immunology-based method, and polymerase chain reaction method. Although these methods are sensitive, inexpensive and can provide both qualitative and quantitative information on the number and nature of microorganism, they are constrained by several drawbacks such as complex operation, specialized instruments and trained personnel required for the tests, and long detection time (2 to 3 days for initial results and 7 to 10 days for confirmation). Therefore, there is a critical need for innovative pathogen-detecting biosensors that are reliable, rapid, accurate, simple, sensitive, selective and cost effective (Velusamy et al., 2010; Mandal, Biswas, Choi, & Pal, 2011).

## 2.1. Conjugated Polymers (CPs)

Biosensor systems based on conjugated polymers (CPs) are attractive due to their easy signal analysis and unique optical properties, for example, color transitions and fluorescence emission change upon external stimuli. The external stimuli can be viruses, bacterial toxins, antigens, pathogens, glucose, enzymes et al (Lee, Yarimaga, Lee, Choi, & Kim, 2011; Chen, Zhou, Peng, & Yoon., 2012). Conjugated polymers are organic macromolecules that have alternating saturated and unsaturated bonds along a backbone chain. The backbone atoms are  $sp^1$  or  $sp^2$  hybridized and possess conjugated  $\pi$  electrons that are delocalized rather than being part of one valence bond. Excitation energy of conjugated  $\pi$  electrons is usually in the visible range and hence the conjugated  $\pi$  electrons are optically active and can provide conductivity and fluorescence in CPs. Changes in intramolecular conformation and intermolecular packing in CPs can induce change in effective conjugation length, resulting in changes in the properties of CPs. The study of structure-properties relationships of CPs has been studied with great interest for the decades (Lebouch et al., 2005). The conjugated polymers that exhibit interesting colorimetric behavior (chromism) in response to external stimuli can be potentially used in biosensor development. Previous studies have demonstrated potential biosensor systems using CPs including graphene (Wu, Chu, Koh, & Li, 2010; Li, Zhang, & Cui, 2015), poly (p-phenyleneethynylene) (Lebouch et al., 2005; Hill, Goswami, Evans, & Schanze, 2012), poly (phenylene vinylene) (Koenen, et al., 2014), polydiacetylene (Charych et al., 1993; Jelinek & Ritenberg, 2013).

## 2.2. Polydiacetylene (PDA)

Polydiacetylenes (PDAs) are one of the most attractive conjugated polymers in developing biosensors (Sun et al., 2010; Chen, Zhou, Peng, & Yoon, 2012; Lee et al., 2014).

PDAs are prepared by photo-polymerization with UV or  $\gamma$ -irradiation from self-assembled diacetylene (DA) monomers. The photo-polymerization is free of catalysts or initiators and results highly pure PDAs. PDAs (640 nm absorption wavelength) undergo a color shift from blue to red (550 nm absorption wavelength) upon environmental stimulation. The blue-to-red transition is visible to the naked eyes (Figure 2.4). The blue-phase PDAs are nonfluorescent, while their red-phase counterparts are fluorescent, which makes polydiacetylenes applicable to fluorescence-based sensor systems (Lee et al., 2014). These characteristics make PDAs particularly attractive in detecting chemical and biological molecules such as influenza virus (Charych et al., 1993), *Escherichia coli* (Oliveiraa, Soaresa, Silva, Andrade, & Medeiros, 2013), other microorganisms (Pindzola, Nguyen, & Reppy, 2006) and proteins (Kolusheva, Kafri, Katz, & Jelinek, 2001).

### 2.2.1 Self- assembled Molecular Structures

Polydiacetylenes (PDAs) are readily prepared by 1,4 addition photo-polymerization of self-assembled colorless diacetylene (DA) monomers with 254nm UV light as shown in Figure 2.3 (Lee et al., 2014). The polymerization only takes place when the DAs are arranged in a lattice with appropriate geometry. This topochemical constraint indicates that polymerization can only occur in solids or other highly ordered structures.

DA ( $R_1-C\equiv C-C\equiv C-R_2$ ) monomers are amphiphilic molecules composed of a polar head group and a hydrophobic tail containing the diacetylene group. This amphiphilic nature renders a convenient self-assembly molecular structure in an aqueous environment as shown in Figure 2.3. Each tail can be broken down into three components: the diacetylene group, a spacer between the head group and the diacetylene, and the terminal alkyl chain. Each element of the diacetylene amphiphile plays a crucial role towards the formation and the properties of the self-assembled

molecular structure. Due to the amphiphilic nature, DAs are likely to form intermolecular (between DA monomers) packing in water via hydrophobic-hydrophobic interactions of adjacent tails of DAs. Furthermore, hydrophilic head groups such as carboxylic acid or amide groups in DAs can also form intermolecular hydrogen bonding. The aromatic head groups of DAs can promote  $\pi$ - $\pi$  stacking interactions that stabilize the self-assembled structure of DAs.

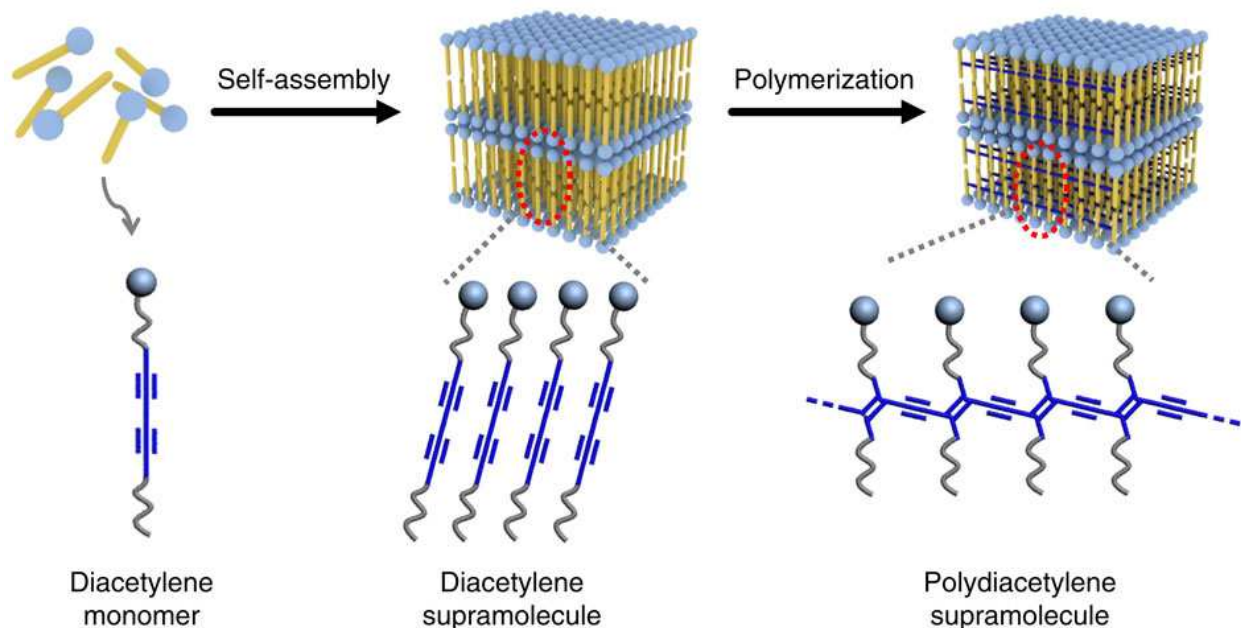


Figure 2-3 Polymerization of DA monomer (Lee et al., 2014).

### 2.2.2 Colorimetric Transition

PDA shows either a blue or a red color, depending on the polymerization conditions. The origin of the color difference is not well understood. In 1984, Wegner et al. summarized the relationship between the wavelength of the absorbance and the effective conjugation length (ECL) in PDAs (Wenz, Mueller, Schmidt, & Wegner, 1984). They found that ECL is strongly affected by the planarity of the main chain of PDA in a linear relationship. They explained that the PDAs with an ECL of around 20 monomers show a red color and the PDAs with an ECL of 30 monomers show a blue color. The ECL is determined by the degree of p-orbital overlap. The

smaller the energy gap between the valence and conduction bands, the longer the ECL. PDA has its absorption at around 650 nm showing blue color after polymerization (*Figure 2.4*). When the blue phase PDA is exposed to external stimuli (pH, temperature, mechanical stress, microorganism etc.), the conjugated backbone of the PDA becomes twisted and non-planar p-orbitals overlap. The changes reduce the conjugation length and increase the energy band gap in the PDA molecules. As a result, the PDAs absorb at around 550 nm and become red.

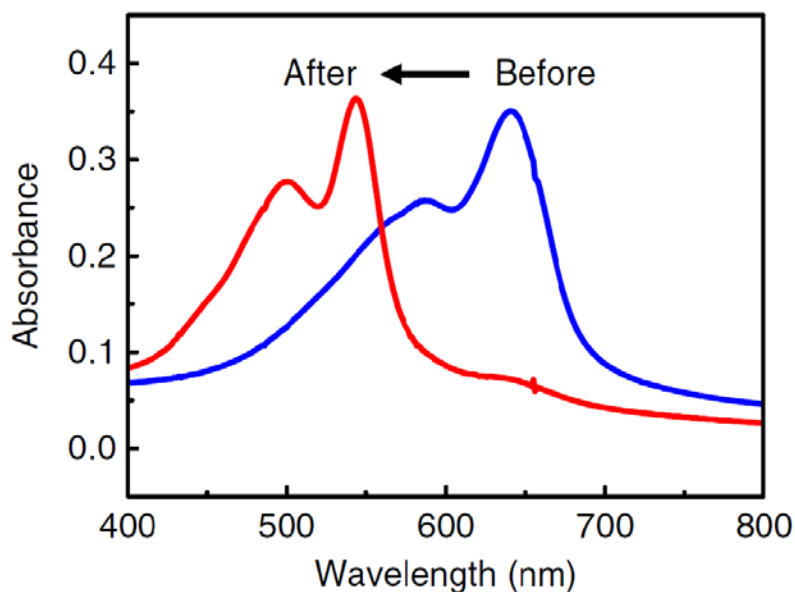


Figure 2-4 Absorption spectral and color changes of a PDA solution that take place upon stimulation. (Ahn and Kim, 2008)

### 2.2.3. PDA Nanofibers

PDAs have been mixed with other polymers to create responsive polymer composites. For example, PDA is embedded in polyethylene oxide (PEO) and then electrospun into PDA-PEO nanofibers (Chae et al., 2007; Yoon, Chae, & Kim, 2007; Jeon, Lee, Kim, & Yoon, 2012). The PEO is used as a matrix polymer to increase the viscosity of the PCDA solution in chloroform so that the PEO-PCDA solution is spinnable. PEO is a biocompatible polymer and approved for internal use in food, cosmetics, pharmaceuticals and personal care. PEO has great

potential for biosensor application due to its excellent biocompatibility (Bhattarai, Edmondson, Veisheh, Matsen, & Zhang, 2005). PDA electrospun nanofibers are also made with polymethyl methacrylate (PMMA) (Chae et al., 2007) and tetraethyl orthosilicate (TEOS) (Yoon, Chae, & Kim, 2007) for chemosensor application. PDA nanofibers are an average 100 nm in diameter and can be used for sensor applications. The high surface area to volume ratio of the nanofibers provides an increased number of sites for analyte interaction or signal transduction, resulting in high sensitivity as well as a short response time (Steyaert, Rahier, & De Clerck, 2015).

#### 2.2.4. Electrospinning Apparatus

A typical electrospinning apparatus is shown in Figure 2.5. It consists of four major components: a high voltage DC power supply, a syringe pump, a spinneret, and a grounded collector. The system utilizes a high voltage DC power source, in the range of several tens of KV, to inject charge of a certain polarity into a polymer solution or melt, which is then accelerated towards a collector of opposite polarity (Bhardwaj & Kundu, 2010; Liang, Hsiao, & Chu, 2007). Electrospinning is conducted at room temperature with standard atmospheric conditions (Li & Xia, 2004).

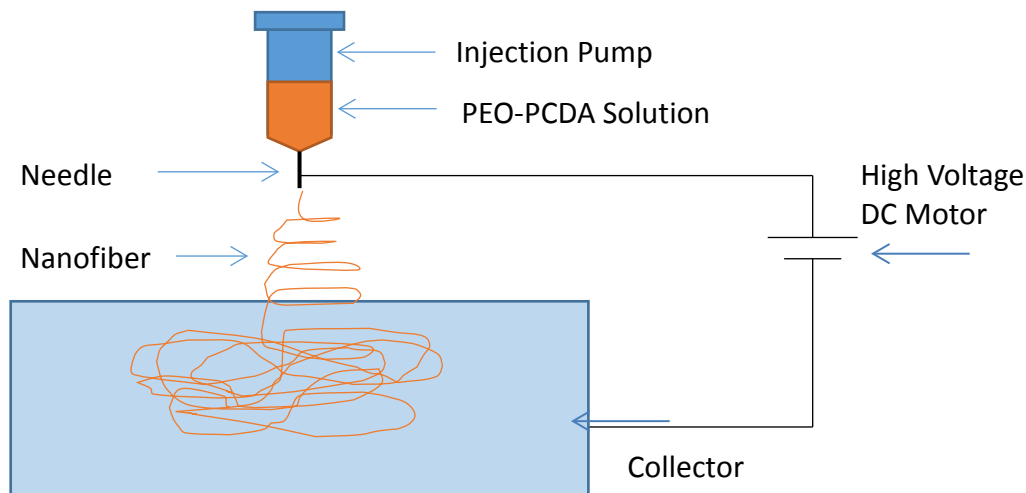


Figure 2-5 Schematic set up of a basic vertical electrospinner

### **2.2.5. Electrospinning Parameters**

The electrospinning process is governed by many parameters, classified broadly into solution parameters, process parameters, and ambient parameters (Nandana & Kundu, 2010). Solution parameters include viscosity, conductivity, molecular weight, and surface tension. Process parameters include applied electric field, tip to collector distance, and feeding or flow rate. The ambient parameters include temperature and relative humidity of the spinning room. Each of these parameters significantly affects the fiber morphology, and by proper manipulation of these parameters, nanofibers of desired morphology and diameters can be obtained (Nandana & Kundu, 2010).

### **2.2.6. Solution Parameters**

Polymer molecular weight reflects the number of entanglements of polymer chains in a solution, and thus solution viscosity. Molecular weight of the polymer has a significant effect on rheological and electrical properties such as viscosity, surface tension, conductivity, and dielectric strength (Haghi & Akbari, 2007). Generally, too low molecular weight solution tends to form beads rather than fibers, and a high molecular weight solution gives fibers with larger average diameters (Nandana & Kundu, 2010).

There is an optimum solution concentration for the electrospinning process. It has been found that at a low solution concentration, a mixture of beads and fibers is obtained and as the solution concentration increases, uniform fibers with increased diameters are formed because of the higher viscosity (Haghi & Akbari, 2007; Mckee, Wilkes, Colby, & Long, 2004).

Surface tension, which is a function of solvent, plays a critical role in the electrospinning process (Hohman, Shin, Rutledge, & Brenner, 2001). High surface tension of a solution inhibits electrospinning (Haghi & Akbari, 2007), and by reducing surface tension bead-less fibers can be

obtained (Hohman, Shin, Rutledge, & Brenner, 2001). A lower surface tension of the spinning solution helps electrospinning to occur at a lower electric field (Haghi & Akbari, 2007) although lowering the surface tension of a solvent will not always be more suitable for electrospinning. Basically, surface tension determines the upper and lower boundaries of the electrospinning window, if all other variables are held constant (Pham, Sharma, & Mikos, 2006).

### **2.2.7. Process Parameters**

Applied electric force is the most crucial parameter on which the morphology of the electro spun nanofiber depends although there is some dispute about the role of electric force in the electrospinning process (Nandana & Kundu, 2010). Reneker and Chun (1996) demonstrated that there is not much effect of electric field on the fiber size when electrospinning with polyethylene oxide. At higher voltages, more polymer is ejected which leads to the formation of a larger diameter fiber (Demir, Yilgor, Yilgor, & Erman, 2002; Zhang, Yuan, Wu, Han, & Sheng, 2005). However, other authors (Buchko, Chen, Shen, & Martin, 1999; Yuan, Zhang, Dong, & Sheng, 2004) have reported that an increase in the applied voltage increases the electrostatic repulsive force on the fluid jet, which ultimately favors finer fiber. Larrondo and Manley (1981) showed that doubling the applied voltage decreases the fiber diameter by roughly one-half.

The injection speed is one of the most important parameters as it influences the jet velocity and the material infusion rate. Bhardwaj and Kundu (2010) reported that the fiber diameter increases with an increase in the polymer injection rate. At a lower injection rate the solvent has enough time for evaporation (Yuan et al., 2004); conversely, a high injection rate results in beaded fibers since proper drying time does not occur prior to reaching the collector

(Yuan et al., 2004). However, there should be an optimum distance that favors solvent evaporation, and provides sufficient time to drying (Geng et al., 2005).

### **2.2.8. Ambient Conditions**

Besides the solution parameters and spinning parameters, the relative humidity and temperature also affect electrospinning (Bhardwaj & Kundu, 2010). Li and Xia (2004) observed that high humidity can help the formation of the electrospun fibers. At very low humidity, volatile solvents may dry up rapidly due to the faster evaporation of the solvent. On the other hand, an increase in the humidity results in the appearance of small circular pores on the surface of the fibers (Casper, Stephens, Tassi, Chase, & Rabolt, 2004). In a study on the effect of temperatures ranging from 25<sup>0</sup>C to 60<sup>0</sup>C, Mit-uppatham, Nithitanakul, & Supaphol (2004) found an inverse relation between temperature and fiber diameter. They attributed the decline in fiber diameter at an increased temperature to the decrease in the viscosity of polymer solution.

### **2.3. Color Analysis**

CIE LAB is an internationally recognized method for quantifying color appearance. It was developed by the Commission International D'Eclairage (Weatherall & Coombs, 1992). The CIE LAB software characterizes color in a three-dimensional space as shown in Figure 2.6. The vertical axis (L\*) is the lightness/darkness indicator. It ranges from 0 (Black) to 100 (White). Any value up to 50 indicate a darker sample, whereas values above 50 indicate a lighter sample. One horizontal axis ranges from blue (negative b\* values) to yellow (positive b\* values). The other horizontal axis ranges from green (negative a\* values) to red (positive a\* values) (Weatherall & Coombs, 1992; Yoshida, Yoshioka, Inoue, Takaichi, & Maeda, 2007).  $\Delta E^*$  indicates the color difference between objects, hence  $\Delta E^*$  can be used to compare color changes between objects.  $\Delta E^*$  is defined by the following equation:

$$\Delta E^* = [(\Delta L^*)^2 + (\Delta a^*)^2 + (\Delta b^*)^2]^{1/2}$$

where  $\Delta L^*$ ,  $\Delta a^*$ , and  $\Delta b^*$  are differences in  $L^*$ ,  $a^*$ , and  $b^*$  values between objects.

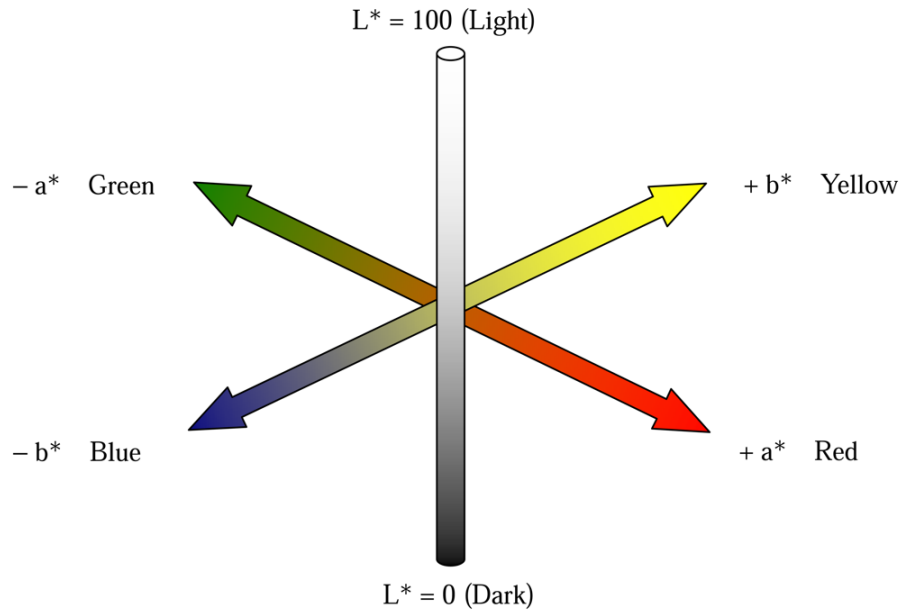


Figure 2-6 Graphical representation of the CIELAB  $L^*$ ,  $a^*$ ,  $b^*$  value three dimensional space (Adobe Systems Incorporated, 2000)

$K/S$  values are used to evaluate the strength (depth) of the color, and are calculated using the Kubelka and Munk equation (Sarker and Seal, 2003; Yoshida ,Yoshioka , Inoue, Takaichi, & Maeda, 2007). The equation is as follows:

$$\frac{K}{S} = \frac{(1 - R)^2}{2R}$$

Where  $R$  is the reflectance coefficient,  $K$  is the absorption coefficient and  $S$  is the scattering coefficient. Large  $K/S$  values indicates deep color. Sarker and Seal (2003) used the Kubelka and Munk equation to examine color strength of flax fabrics dyed with natural dyes; Yoshioka ,Yoshioka , Inoue, Takaichi, & Maeda (2007) used  $K/S$  values to evaluate differences between colors of the bacterial cultures.

## CHAPTER 3. MATERIALS AND METHODS

### 3.1 Materials

10, 12-Pentacosadiynoic acid (PCDA, 98 %) was purchased from GFS Organics (Columbus, OH, USA) and was used as monomer to prepare polydiacetylene (PDA). Polyethylene oxide (PEO,  $M_w = 300,000 \text{ g mol}^{-1}$ ) was purchased from Sigma-Aldrich (St. Louis, MO, USA). PEO was used as matrix polymer for fiber formation. Chloroform ( $\geq 99.8 \%$ ) was purchased from Sigma-Aldrich (St. Louis, MO, USA), and was used as solvent for electrospinning solution preparation. Diethyl ether was purchased from Fisher Scientific (Fair Lawn, NJ, USA). All the polymers and solvents were used without further purification.

### 3.2 Methods

#### 3.2.1 Preparation of PDA

The diacetylene monomer PCDA (6.44 g, 17.2 mmol) was dissolved in diethyl ether (35 mL) and filtered to remove any contaminants. The monomer was isolated after evaporation of the solvent under vacuum in a flask protected from direct exposure to light. Millipore water ( $18.2 \text{ M}\Omega\cdot\text{cm}$ ) was added to yield a 1.29 % weight/volume (w/v) suspension, which was sonicated at  $65 \text{ }^\circ\text{C}$  for 30 min. The suspension was allowed to cool to room temperature, then stored at  $4 \text{ }^\circ\text{C}$  overnight. The suspension was transferred to a crystallizing dish with a magnetic stir bar and irradiated with UV light (254 nm) for 8 min (Champaiboon, Tumcharern, Potisatityuenyong, Wacharasindhu, & Sukwattanasinitt, 2009). After photo-polymerization, the dark blue suspension was transferred to a round bottom flask protected from light to remove the solvent under vacuum. The solid PDA was then stored at  $4 \text{ }^\circ\text{C}$  and characterized by FT-IR.  $^1\text{H}$  NMR

(Proton nuclear magnetic resonance) characterization was not possible due to the impaired solubility of the material.

### **3.2.2 PDA Fiber Composites**

Mixtures of PEO and PCDA in chloroform were prepared at different mass ratios of matrix polymer (PEO) to PCDA (w/w %), different polymer (PEO and PCDA) concentrations, and different injection speeds. Table 1 (manuscript-1) shows the experimental design for preparing PDA fiber composites (PEO-PDA) for electrospinning. A solution of PEO-PDA fibers was prepared by adding the required amount of PEO and PCDA in chloroform, followed by stirring overnight at room temperature on a hotplate stirrer at 350 revolutions per minute (rpm) until a homogeneous light-pink solution was obtained. A customized electrospinning apparatus was used to prepare fibers. The apparatus primarily consisted of a Gamma High Voltage Research ES50P power supply and a Harvard PHD 2000 syringe pump. The uniform electrospinning solution was injected at a constant injection speed ( $0.1 \text{ mL}\cdot\text{h}^{-1}$  or  $0.2 \text{ mL}\cdot\text{h}^{-1}$ ) and 15 KV electrical force. The spinning time was kept constant for 1 hour to obtain a thick, colorless fiber mat. The fibers were collected at a distance of 17 cm on an aluminum collector plate. The obtained fibers were kept in the dark overnight before UV-light (Spectroline, Longlife<sup>TM</sup> filter, New York, USA) irradiation. During irradiation with UV-light at 254 nm, the fibers became blue within 30 s and then turned deep blue in 3 min, indicating photopolymerization of PDA fiber composites.

### **3.2.3 Fiber Characterization**

Fiber size and morphology was studied using scanning electron microscope (JEOL, JSM 6500F, Tokyo, Japan). The fiber samples were kept overnight under vacuum to evaporate any

residual solvent or moisture. Then they were sputter-coated with gold to improve conductivity of the samples for better quality imaging.

FTIR-attenuated total reflectance (ATR) spectra of PDA powders and PEO-PDA fibers were recorded in the range of 650–4000  $\text{cm}^{-1}$  using a Nicolet 6700 FTIR spectrometer (Thermo Electron Corporation, Madison, WI, USA). All materials were dried in a vacuum oven overnight at room temperature prior to the analysis. Two spectra were collected for each of the blue and red phase PDA powders, and PEO-PDA fiber composites. The color change to red was induced by heating both the blue PDA powders and fibers at 120 °C for 10 minutes.

Differential scanning calorimetry (TA Q20 DSC) was used to determine the thermal transitions of the PEO-PDA fibers. The transitions were measured through three heating cycles under nitrogen flow. During the first heating cycle, the temperature was equilibrated at 40 °C and ramped at 10 °C/min to 250 °C and equilibrated at 250 °C. In the second cycle, the temperature was ramped at 10 °C/min to –60 °C and equilibrated at –60 °C. For the third and final cycle, the temperature was ramped at 10 °C/min to 250 °C and equilibrated at 250 °C. A Thermolyne benchtop furnace (Thermolyne, Thermo Fisher Scientific, Waltham, MA, USA) was used for exposing the fibers to treatment temperatures up to 120 °C.

#### **3.2.4. Colorimetric Transition due to Temperature**

Colorimetric transition behavior of the PEO-PDA fibers was evaluated as a function of treatment temperature (25 °C, 50 °C, 60 °C, 70 °C, 80 °C, 90 °C, 100 °C, 110 °C, and 120 °C). The color of PEO-PDA fibers was measured using a spectrophotometer (HunterLab ColorQuest XE). Electrospun fiber mat samples (1 inch  $\times$  1 inch) were first treated in the benchtop furnace for 10 min at 25 °C. The fiber mat was then measured in the spectrophotometer and reflectance spectra were collected from 400 nm to 700 nm. The same fiber mat was later stored back to the

furnace and treated at a higher temperature for another 10 min, followed by reflectance measurement of the fiber mat. Reflectance spectra was collected for the same fiber mat after each heat treatment from 25 °C to 120 °C. For a given fiber mat treated at a given temperature, three spectrophotometric measurements were taken and the average reflectance was used for color analysis.

## CHAPTER 4.MANUSCRIPT

### Study of Polydiacetylene-Poly (Ethylene Oxide) Electrospun Fibers Used as Biosensors

#### SYNOPSIS

Polydiacetylene (PDA) is an attractive conjugated material for use in biosensors due to its unique characteristic of undergoing a blue-to-red color change in response to external stimuli. 10,12-Pentacosadiynoic acid (PCDA) and poly (ethylene oxide) (PEO) were used in this study to develop fiber composites via an electrospinning method at various mass ratios of PEO to PCDA, solution concentrations, and injection speeds. The PEO-PDA fibers in blue phase were obtained via photo-polymerization upon UV-light irradiation. High mass ratios of PEO to PCDA, low polymer concentrations of spinning solution, and low injection speeds promoted fine fibers with small diameters and smooth surfaces. The colorimetric transition of the fibers was investigated when the fibers were heated at temperatures ranging from 25 °C to 120 °C. A color switch from blue to red in the fibers was observed when the fibers were heated at temperatures greater than 60 °C. The color transition was more sensitive in the fibers made with a low mass ratio of PEO to PCDA due to high fraction of PDA in the fibers. The large diameter fibers also promoted the color switch due to high reflectance area in the fibers. All of the fibers were analyzed using Fourier transform infrared spectroscopy (FT-IR) and differential scanning calorimetry (DSC) and compared before and after the color change occurred. The colorimetric transitional mechanism is proposed to occur due to conformational changes in the PDA macromolecules.<sup>1</sup>

---

<sup>1</sup> A version of this manuscript has been published in Materials journal with the following citation details: Alam, A. K. M., Yapor, J. P., Reynolds, M. M., & Li, Y. V. (2016). Study of Polydiacetylene-Poly (Ethylene Oxide) Electrospun Fibers Used as Biosensors. *Materials*, 9(3), 202.

## 1. Introduction

When biomaterials are analyzed using biosensors, biological responses can be converted by the biosensor into measurable signals, providing analytic tools for the compositions, structures, and functions of the biomaterials [1,2]. Ideal biosensors can provide short response time, high precision and accuracy, and painless diagnosis in both *in vitro* and *in vivo* applications including infectious disease monitoring, food safety, environmental monitoring, and military biodefense [3]. One promising application of biosensors is to detect pathogens and bacterial infections in hygiene processes, such as wound care and personal care. Current wound care management of pathogen infection may be time-consuming because it usually requires multiple steps including physical examination, imaging of the wound, and sample testing, sometimes resulting in a delay of treatment [4]. Such a delay could be life-threatening in chronic wound management. Quick and easy pathogen-detecting biosensors are, therefore, greatly needed in wound care [5,6]. Recently, conjugated polymers have gained interest in biosensor development because they exhibit reliable bio-sensing activities, which are usually associated with color transitional behaviors [7,8]. Conjugated polymers, thus, potentially provide easy signal analysis, user friendliness, and painless diagnosis in the biosensor development.

Polydiacetylene (PDA) is one of the attractive conjugated polymers with color transitional properties. PDAs can be prepared by catalysts-free photo-polymerization, resulting in a highly pure product [7,8]. The PDAs usually have absorption at 650 nm, exhibiting a blue color [7]. When the blue phase PDAs are exposed to external stimuli such as chemical or mechanical stress, the absorption is switched to 550 nm and the color of PDAs becomes red [7,9]. The blue-to-red transformation is visible to the naked eye, which makes PDAs attractive materials for biosensor applications. The color transition is also observed when biological factors are applied

to the PDAs, including microorganisms [10] and proteins [11]. Because the sensitivity of sensing activities is important in the use of biosensors, PDAs in different structures have been studied, such as thin films [12–15], crystals [16], coatings, and fibers [17–19], suggesting that the sensitivity is usually greater with an increase in contact surface area. One promising fabrication method that provides high surface areas for sensor materials is electrospinning. In electrospinning, a spinning fluid containing PDA is placed in a syringe loaded on a syringe pump. When a high voltage power is on, an electrostatic force overcomes the surface tension of the spinning fluid to eject a liquid jet from the tip of the syringe needle. The jet then undergoes a stretching process and is eventually deposited on a collector, forming solidified PDA fibers [17]. Yoon *et al.* [18] prepared electrospun fiber mats of PDAs for detecting volatile organic compounds (VOCs) via the blue-to-red color switch. The similar method was also used to make PDA fibers for detecting tracer HCl gas, suggesting a significant sensitivity of PDA-containing electrospun fibers. The color change of PDA electrospun fibers was compared with thin films prepared from the same solution, and PDA fibers exhibited superior sensitivity over the PDA films [20]. The high surface area to volume ratio of the electrospun fibers provided an increased number of sites that interacted with external factors, resulting in high sensitivity and a shorter response time, which is favorable for biosensor applications [21]. Electrospinning of PDAs without another polymer is challenging because the viscosity of PDA solutions is relatively low [18]. When mixed with another polymer that is able to increase the viscosity of the spinning solution, PDAs can be incorporated into fiber composites via electrospinning. The other polymer serves as a supportive component in the fiber composites and hence is named the matrix polymer. Previously, PDA electrospun fibers have been developed with matrix polymers such as

polymethyl methacrylate (PMMA) [17,18], polystyrene (PS) [18], tetraethyl orthosilicate (TEOS) [22], and poly (ethylene oxide) (PEO) [17].

We have developed PDA fiber composites and observed a blue-to-red color switch in the composites when they were immersed in bacterial solution at room temperature. The observation suggested a great potential for the PDA composites to be used as biosensors. However, previous discussion indicates that the color switch may be due to other external factors such as temperature. Although it is known that PDAs exhibit a color switch at high temperature [7], little is known on the relationship between the temperature and the colorimetric transition in a PDA-embedded fiber composite. If the PDA fiber composite is used in a biosensor, it is critical to determine if a colorimetric transition is triggered by the change in temperature or by the presence of bacteria in the environment. This paper presents a study on the development of PEO-PDA fiber composites and their colorimetric transition properties as a function of temperature, potentially used in the biosensors for wound dressings. In this study, PEO was used as the matrix polymer because it has excellent biocompatibility and is often used in internal applications of food, pharmaceutical and personal care products [23]. PEO was mixed with 10, 12-pentacosadiynoic acid (PCDA) in the electrospinning solution. The PCDA was photopolymerized upon UV-light irradiation resulting in PEO-PDA fibers. Electrospinning parameters including polymer concentration, mass ratio of PEO to PCDA in solution, and injection speed were studied. The PEO-PDA fibers were obtained with diameters ranging from 220 nm to 3.4  $\mu\text{m}$ . Colorimetric transitional properties of the obtained PEO-PDA fibers were evaluated using a spectrophotometer and compared before and after the fibers were exposed to temperatures ranging from 25 °C to 120 °C. The colorimetric transition in response to temperatures changes varied in the fibers depending on how the fibers were made. The blue-to-red switch was not

observed in the fibers until the temperature was more than 60 °C. The results were meaningful because an optimum temperature where bacterial growth in wounds is most rapid and luxuriant is usually 35–37 °C [24]. It suggested that the PEO-PDA fiber composite could be potentially used in wound dressings at normal body temperature range (35–37 °C), directly for detecting biological change, such as bacterial infection. Thermal and chemical properties of the fibers were also analyzed using differential scanning calorimetry (DSC) and Fourier transform infrared spectroscopy (FT-R) to gain an understanding of the color transition mechanism of the fibers. The results revealed a conformational change involving C-C bond rotation in the PDA macromolecules after the heat treatments. It is hypothesized that the conformational change of the PDA leads to the color change from blue to red in PEO-PDA fibers.

## **2. Results and Discussion**

### **2.1. Preparation of PEO-PDA Fibers**

Mixture solutions of PEO and PCDA in chloroform were prepared with varied mass ratios of PEO to PCDA (2, 3, and 4 in Table 1). The solutions were injected by a syringe pump at 0.1 mL h<sup>-1</sup> (or 0.2 mL h<sup>-1</sup>) and at 15 kV. PEO-PDA fibers in nano and submicron size were obtained on a flat collector placed at a distance of 17 cm. The synthetic scheme of PDA containing fibers is illustrated in Figure 4-1. When the mixture of PEO and PCDA was stretched during the electrospinning, there were larger attractive forces between the PCDA monomers than those between the PCDA and the PEO matrix, resulting self-assemblies of the PCDA monomers in the obtained fibers. The self-assembled PCDA monomers were then polymerized when the fibers were treated with UV-light irradiation. The fibers were colorless before the UV-light treatment and then became blue upon the UV-light irradiation, suggesting that the PCDA monomers were polymerized to produce PDAs embedded in the fibers [17].

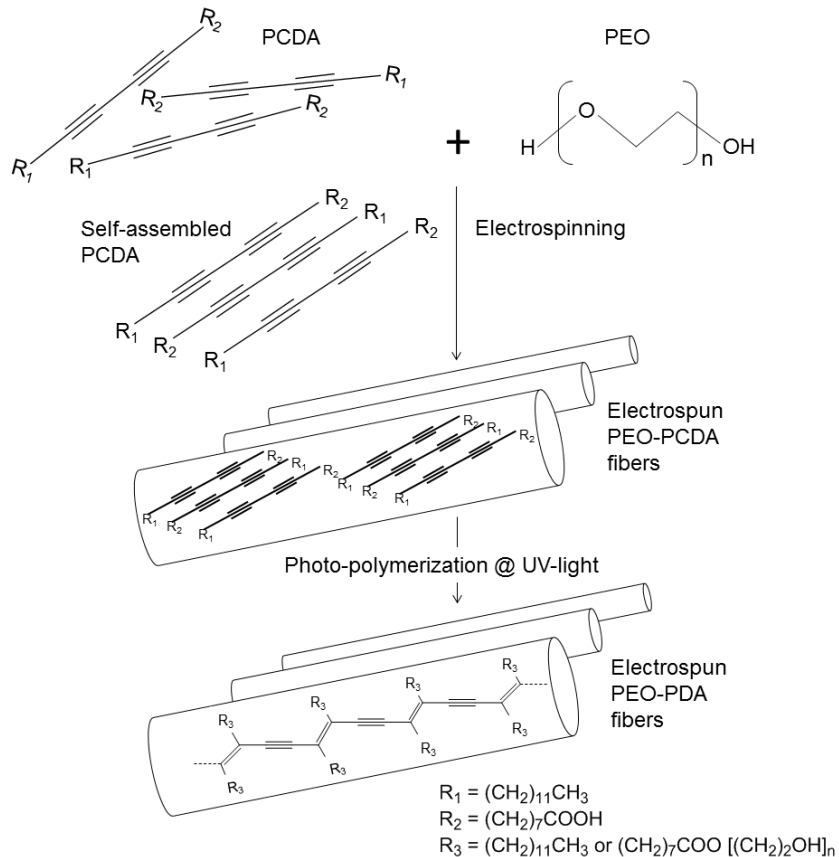


Figure 4-1 Schematic representation of the electrospinning of poly (ethylene oxide) (PEO) –Polydiacetylene (PDA) composite fibers.

## 2.2. Characterization of Fiber Morphology

It was found that the electrospinning parameters of polymer solution concentration, mass ratios of PEO to PCDA, and injection speed had great impact on the morphology of the PEO-PDA fibers. Figure 4-2 shows average diameters of the fibers prepared at varied parameters using electrospinning. Fine fibers were obtained at high mass ratios of PEO to PCDA, because more PEO in the mixture was able to enhance the fiber formation due to the higher viscosity of PEO supporting fiber stretchability. As expected, the low injection speed ( $0.1 \text{ mL h}^{-1}$ ) produced fine fibers because the amount of polymer solution injected to the spinning region was smaller, resulting finer fibers. Fiber diameters increased with the increase in polymer concentration. The

increase in polymer concentration usually prevents rapid changes in the Taylor cone zone of electrospinning, resulting in thick and uniform fibers.

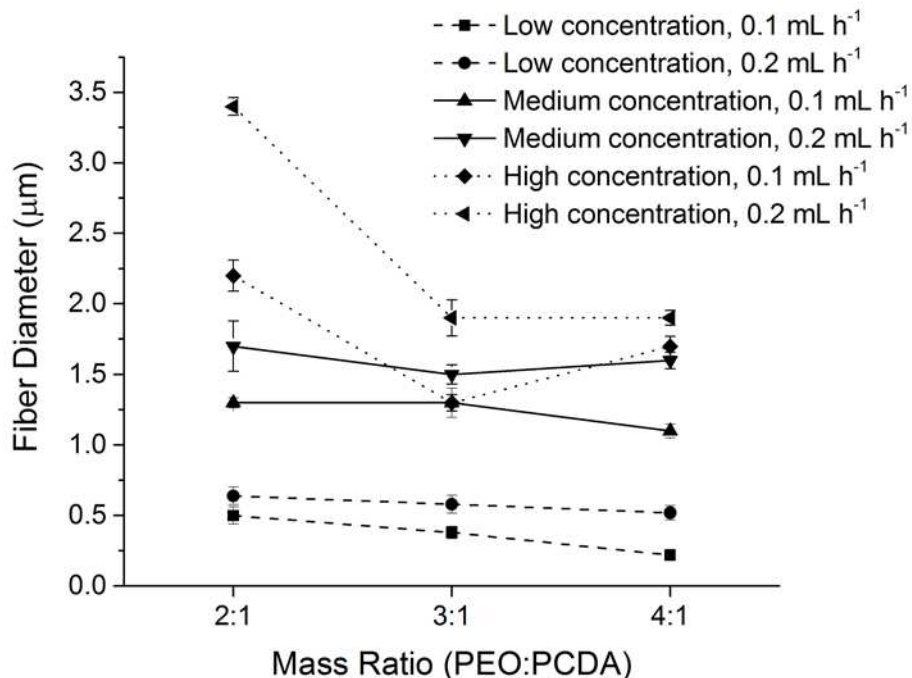


Figure 4-2 Fiber diameters are illustrated as a function of polymer concentration, mass ratios of PEO and PCDA, and injection speed. The injection speed used was 0.1 mL h<sup>-1</sup> (■, ▲, ◆) and 0.2 mL h<sup>-1</sup> (●, ▼, ◄), respectively. Finer fibers were formed at higher mass ratios, lower concentrations, and lower injection speeds.

SEM images of the electrospun fibers, shown in Figure 4-3, illustrate the variation in fiber morphology. The fibers obtained at low concentrations contained beads and junctions (Figure 4-3A-F). Also, there were more beads in the fibers obtained at a low injection speed (Figure 4-3A, C, and E). The amount of beads on fibers was reduced with an increase of both polymer concentration and injection speed. When the polymer concentration was more than 3 wt. % at any mass ratios, bead-free fibers were formed, indicating a critical concentration of 3 wt. % was required in this study for yielding bead-free fibers. The critical concentration allows polymer chain entanglement that is sufficient for the formation of continuous fibers [25,26]. When the

electrically driven polymer jet is elongated in the spinning region, the entanglement of polymer chains prevents them from breaking up, resulting in bead-free fibers.

The surface roughness of the fibers was also varied depending on the electrospinning parameters. High mass ratio of PEO to PCDA promoted fibers with smooth surfaces possibly due to high fraction of PEO in the mixture solution that enhanced fiber formation. It was also found that the surface roughness of the PEO-PDA fibers increased with an increase in solution concentration and injection speed. In previous studies, surface roughness of electrospun fibers containing PDAs was reported to be varied when different solvents were used, including dimethylformamide, chloroform, and methylene chloride [18]. When a mixture of PCDA and poly (methyl methacrylate) (PMMA) in methylene chloride was electrospun, the obtained fibers exhibited porous structures on the surface [17].

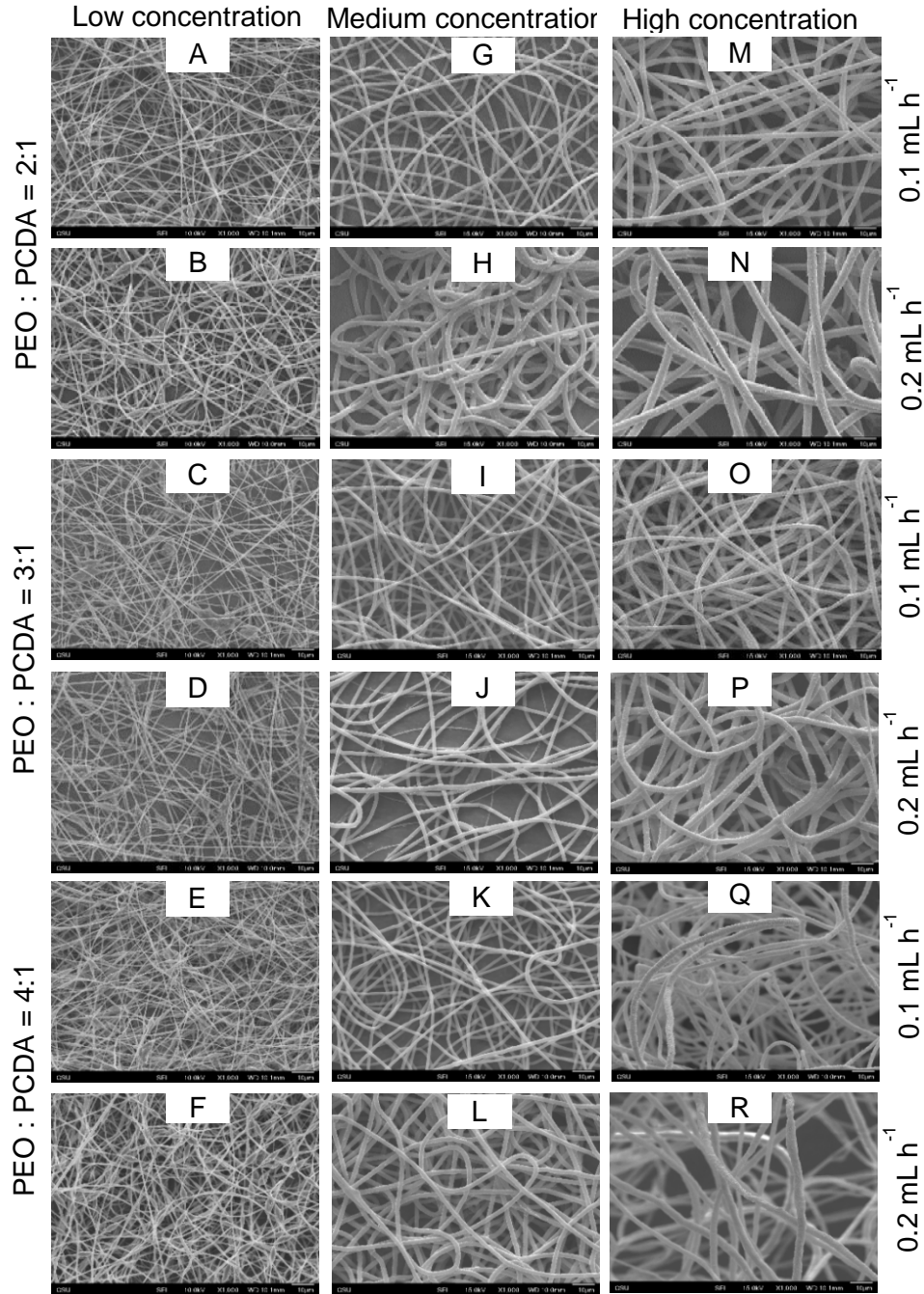


Figure 4-3 SEM images of PEO-PDA electrospun fibers. Fibers presented in first column (A-F), second column (G-L), and third column (M-R) were prepared at low concentrations, medium concentrations, and high concentrations respectively. Respective mass ratio and injection speed are mentioned respective at the left and right side of the fiber images. Fibers with beads were prepared at low concentrations (A-F) irrespective of mass ratio of PEO to PCDA. Number of beads were higher at low ( $0.1 \text{ mL h}^{-1}$ ) injection speed (A, C and E) as compared to the high ( $0.2 \text{ mL h}^{-1}$ ) injection speed (B, D and F). Smooth fibers were developed with an increase in concentration and injection speed.

### 2.3. Temperature Sensitive Properties of PEO-PDA Fibers

Colorimetric transition of the PEO-PDA fibers was evaluated after the fibers were heat-treated at a temperature ranging from 25 °C to 120 °C using a spectrophotometer. 18 PEO-PDA fibers obtained at varied spinning parameters (see Table 1) were all measured using the spectrophotometric method. Representative spectra of fiber #9 are shown in Figure 4-4. The fiber #9 was obtained at 3:1 mass ratio of PEO to PCDA, injection speed of 0.1 mL h<sup>-1</sup>, and polymer solution concentration of 3.34 wt.%. The inserted photographs taken at the different temperatures are associated with the corresponding reflectance spectra of the fiber.

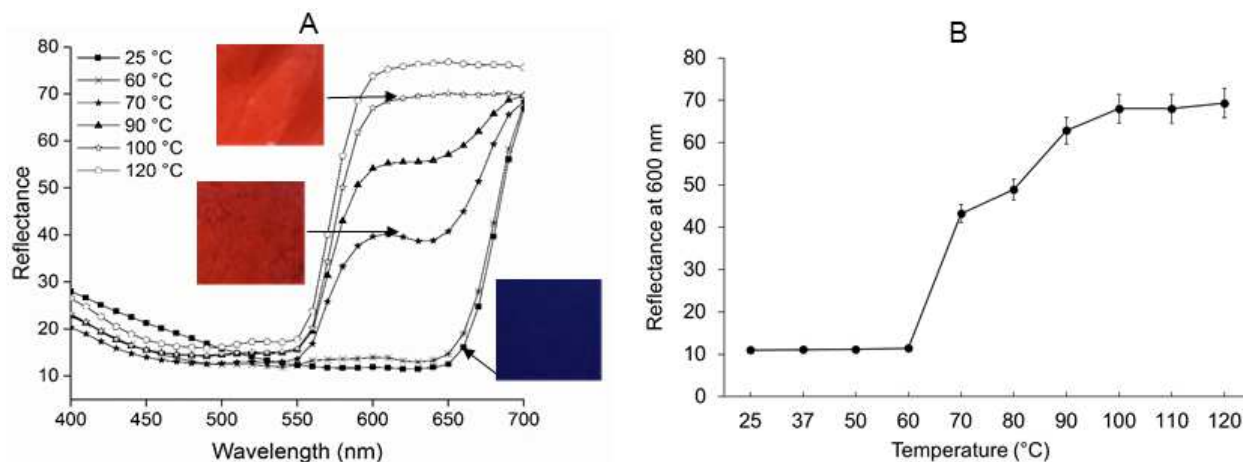


Figure 4-4 (A): Reflectance spectra of the selected PEO-PDA fiber (Fiber #9) treated at selected temperatures (25 °C, 60 °C, 70 °C, 90 °C, 100 °C, and 120 °C). The inserted photographs show the color of the fibers. The fibers treated at 70 °C began to exhibit colorimetric transition on both the reflectance spectra and the photograph. The color switch in the fiber was continuously developed until the temperature was 110 °C. No further change in either reflectance spectra or photograph was observed at 120 °C; (B): Reflectance at 600 nm for the fibers treated at different temperature is plotted as a function of temperature ranging from 25 °C to 120 °C. The same color switch behavior was clearly observed when the temperature was more than 60 °C.

The fiber exhibited arising and high reflectance at 650 nm to 700 nm at low temperatures (37 °C and 50 °C) and a blue color in the corresponding photograph. When the heat treatment continued for the fiber, the fiber began to demonstrate a reflectance switch to a lower wavelength

at 550 nm from 700 nm, resulting in a red color in the corresponding photograph. The reflectance switch was observed in all of the fibers studied in this work, but did not occur until the temperature was more than 60 °C for most of the fibers. It was much significant when the temperature reached 70 °C for all of the fibers (#1–#18). The observation that no blue-to-red switch occurred at low temperatures in the range of normal body temperature could exclude a false positive signal for biological sensing applications, such as bacterial infection.

Normalized reflectance spectra of all the fibers heated at 70 °C are presented in Figure 4-5 where the diameters of the corresponding fibers are also inserted. The fibers with mass ratio of PEO to PCDA of 2:1 (see Figure 4-5A) clearly showed a more pronounced reflectance switch (color transition of blue to red) than the fibers with mass ratios of 3:1 and 4:1 (see Figure 4-5B, 4-5C). There was 33.33% PDA in the fiber composite with mass ratio of PEO to PCDA of 2:1. This high fraction of PDA in the fiber composite provided high sensitivity of color switch properties of the fiber. It is also interesting that that the reflectance switch was increasingly pronounced with an increase in fiber diameter, particularly for the fibers with 33.33% PDA (mass ratio of PEO to PCDA of 2:1) (see Figure 4-5A). Our early discussion on fiber size indicated that the polymer solution and injection speed influenced the fiber size, resulting in an order of fiber diameter as shown in the inserted plots in Figure 4-5A. The high reflectance associated with the coarse fibers was possibly due to high reflectance surface area. The reflectance switch, or color transition, continuously developed when the temperature was more than 70 °C, but no further change was found after the temperature was more than 110 °C, suggesting that an equilibrium was reached in the PDA macromolecule structure.

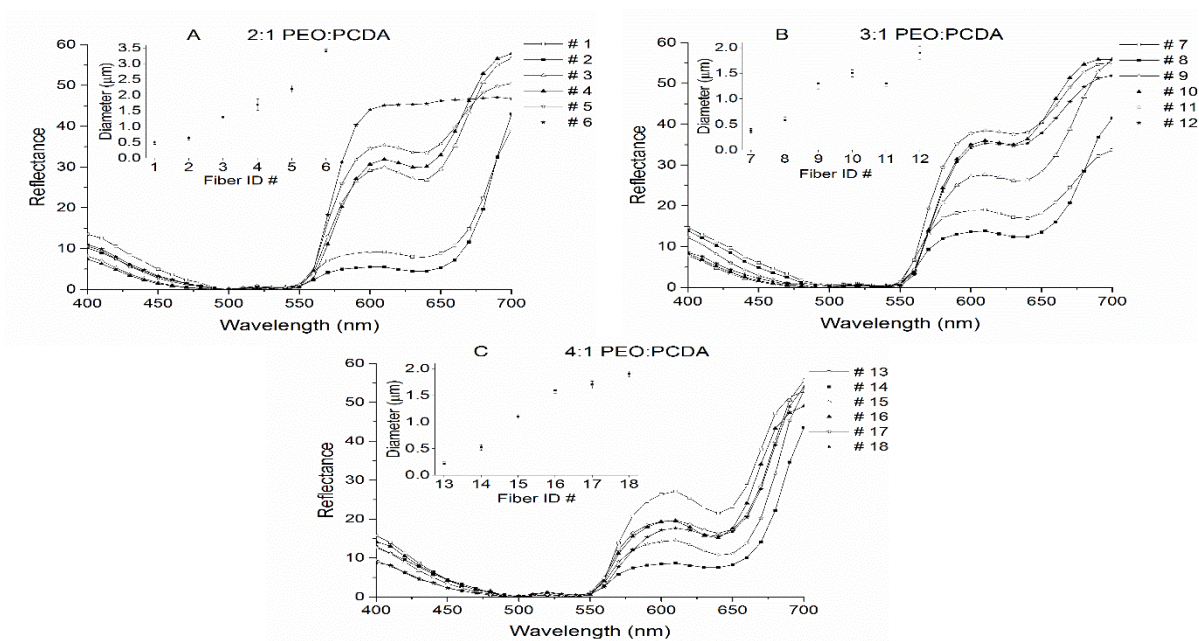


Figure 4-5 Normalized reflectance spectra of 18 fibers that were heated at 70 °C for 10 minutes. **(A)** Fibers #1–#6 have mass ratio of PEO to PCDA of 2:1; **(B)**: Fibers #7–#12 have mass ratio of PEO to PCDA of 3:1; **(C)**: Fibers #13–#18 have mass ratio of PEO to PCDA of 4:1. The inserted figures show the diameters of the corresponding fibers. Fibers #1–#6 exhibit a more pronounced reflectance switch from blue to red.

The blue and red PEO-PDA fibers were compared in FTIR analysis. The results shown in Figure 4-6 indicate the presence of functional groups expected after the polymerization of PDA in the fibers. Spectrum A corresponds to the blue PEO-PDA fibers, where the following resonance features were interpreted for characterization: IR  $\nu_{\max}/\text{cm}^{-1}$ : 2919  $\text{cm}^{-1}$  (H-C=C), 2885-2848  $\text{cm}^{-1}$  (H-C-H), 1692  $\text{cm}^{-1}$  (C=O, ester), and 1097  $\text{cm}^{-1}$  (C-O). Similar features were observed in the spectrum B of the red PEO-PDA fibers: IR  $\nu_{\max}/\text{cm}^{-1}$  2919  $\text{cm}^{-1}$  (H-C=C), 2885-2857  $\text{cm}^{-1}$  (H-C-H), 1722  $\text{cm}^{-1}$  (C=O, ester), and 1107  $\text{cm}^{-1}$  (C-O). The resulting resonance features were similar to previously reported results for the PDAs [27,28].

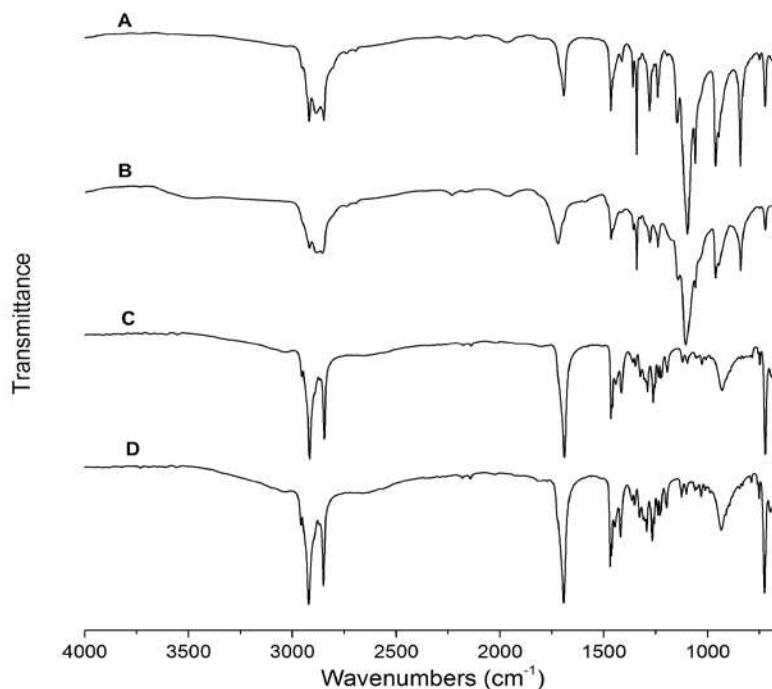


Figure 4-6 Fourier transform infrared spectroscopy (FT-IR) spectra of PEO-PDA fibers and PDA polymers. The signals correspond to: blue PEO-PDA fibers (A), red PEO-PDA fibers (B), blue PDA (C), and red PDA (D).

PDA was also synthesized in the absence of PEO and characterized by FTIR before and after the color transition (Figure 4-6C, 4-6D). Spectrum C represents the blue phase PDA where the following resonance features were observed: IR  $\nu_{\max}/\text{cm}^{-1}$ : 2955  $\text{cm}^{-1}$  (H-C=C), 2918-2847  $\text{cm}^{-1}$  (H-C-H), 1690  $\text{cm}^{-1}$  (C=O, ester), and 722  $\text{cm}^{-1}$  (C=C). Spectroscopic data on spectrum D correspond to the red PDA: IR  $\nu_{\max}/\text{cm}^{-1}$ : 2955  $\text{cm}^{-1}$  (H-C=C), 2918-2847  $\text{cm}^{-1}$  (H-C-H), 1690  $\text{cm}^{-1}$  (C=O, ester), and 722  $\text{cm}^{-1}$  (C=C).

Previous studies suggested the colorimetric change is due to a twist of the conjugated backbone of the PDAs upon high temperature. The changes reduce the conjugation length and increase the energy band gap in the macromolecular structures of PDAs, which is manifested *via* a color switch from blue to red [7,15]. The similarities found in the IR spectra confirm that the PDA retains its functional groups as it transitions from blue to red. A hypothesis based on these

results is that the color change is due to a conformational variation in the side-chains of the PDA which disrupts the  $\pi$  overlap and changes its planarity [29]. This in turn causes changes to the electronic configuration of the PDA, which changes the absorption wavelengths. On spectra A and B, the stretching band associated with the hydrogen-bonded carbonyl shifts from 1692 to 1722  $\text{cm}^{-1}$ , indicating an increase in the C=O bond strength, thus a reduction in the strength of the hydrogen-bond [30]. This suggests that the C-C rotation creates strain on the polymeric backbone and affects the chemical environment surrounding the alkyne and disfavors hydrogen-bonding on the end groups of the polymer. In addition, the resonance band at 1097  $\text{cm}^{-1}$  (A) shifts slightly to 1107  $\text{cm}^{-1}$  (B). This subtle change suggests that the matrix polymer (PEO) is also affected by the induced color change. The matrix polymer might be slightly modified as a result of temperature changes which cause oxidation indicated by the resonance band shifts [31]. However, spectra C and D have almost identical vibrational frequencies for the blue and red phases of PDA, where only very subtle changes can be noticed. One such variation is the vibrational frequency at 931  $\text{cm}^{-1}$  (C-C), which appears to have higher intensity for the red fibers, suggesting that rotational changes cause the transmittance of the peak to vary. These features and spectroscopic data suggest that changes to the conformation may occur within the backbone of the polymer as it is exposed to increased temperature, disrupting the hydrogen-bonding and causing changes in the electronic configuration of the polymer. The IR results also suggest that the matrix PEO in the PEO-PDA fiber composite does not delay or retard the colorimetric transition in the PDA.

Figure 4-7 illustrates DSC analysis results obtained from the second and third cycles of the blue and red PEO-PDA fibers, respectively. The melting temperature ( $T_m$ ) and crystallization temperature ( $T_c$ ) were calculated from the second and third heating cycle, after the thermal history of the mixture of PEO and PDA had been removed. Figure 4-7A shows the data collected from the blue fibers where  $T_c$  was 43.72 °C, and the  $T_m$  was 60.27 °C. Similarly, Figure 4-7B depicts the data from the red fibers where the  $T_c$  was 43.88 °C, and the  $T_m$  was 61.94 °C.

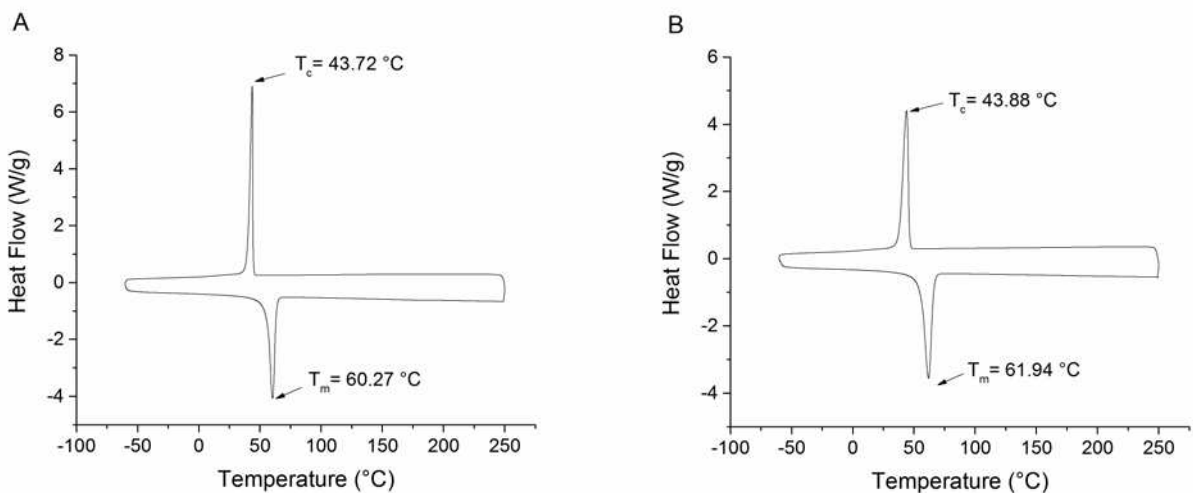


Figure 4-7 Differential scanning calorimetry (DSC) plot of PEO-PDA fibers: (A) blue fibers; and (B) red fibers.

Both the blue and red fibers showed similar crystallization and melting temperatures (Figure 4-7A, 4-7B). The crystallization temperatures were determined during the cooling cycle at 43.72 °C and 43.88 °C for the initially blue and red fibers, respectively. This temperature indicates that the crystalline regions in the PEO-PDA fibers became ordered and crystalline, while the amorphous regions provided flexibility to the fibers. It is noteworthy that the melting temperature falls in the range of 60–70 °C, which is the same as when the occurrence of color transition from blue to red is observed in the fibers, as discussed previously. This consistency supports the hypothesis that the optical properties of the material may be influenced by a structural alignment of the polymer chains. As the temperature is increased, C-C bond rotation is

facilitated and disruption of hydrogen-bond networks may destabilize the planarity of the polymer conformation [32]. A change in the conformation of the material is possible due to the phase change of the fibers that increases the entropy of the system, which is shown in Figure 4-8.

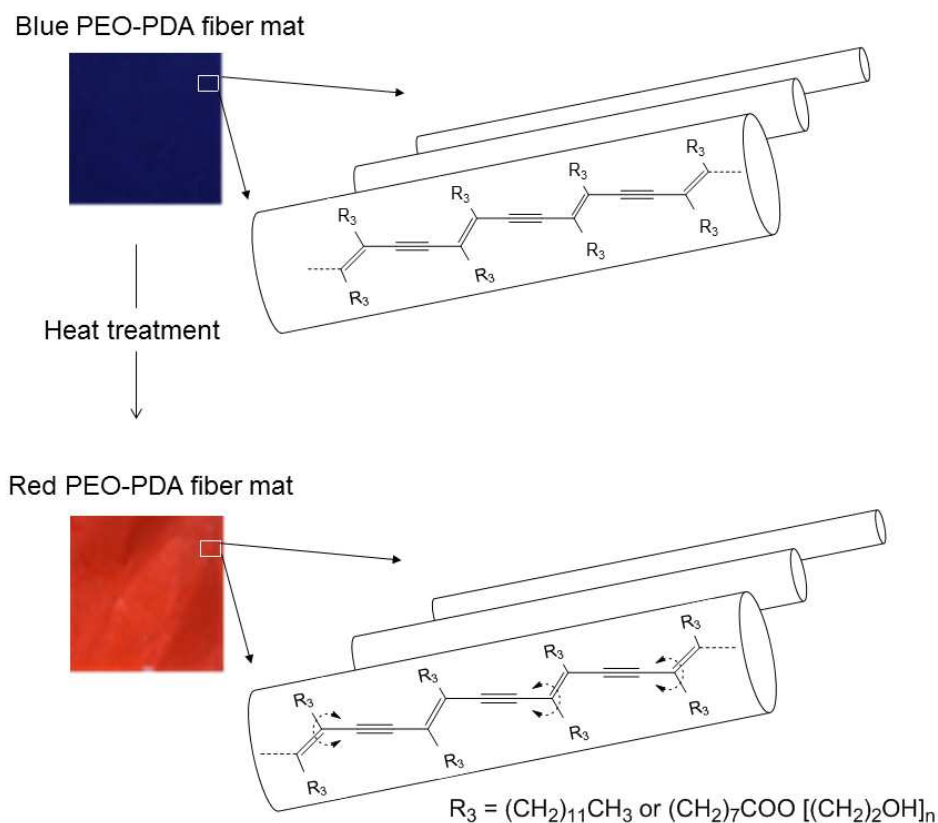


Figure 4-8 An illustration of color transition from blue to red in PEO-PDA fiber mat, which is due to a C-C bond rotation induced by heat treatment.

### 3. Materials and Methods

#### 3.1. Materials

10, 12-Pentacosadiynoic acid (PCDA, 98%) was the monomer used to prepare polydiacetylene (PDA) and was purchased from GFS Organics (Columbus, Ohio, USA). Polyethylene oxide (PEO,  $M_w = 300,000 \text{ g mol}^{-1}$ ). Chloroform ( $\geq 99.8\%$ ) was purchased from

Sigma-Aldrich (St. Louis, MO, USA). Diethyl ether was purchased from Fisher Scientific (Fair Lawn, NJ, USA).

## **3.2. Methods**

### **3.2.1. Preparation of PDA**

The diacetylene monomer PCDA (6.44 g, 17.2 mmol) was dissolved in diethyl ether (35 mL) and filtered to remove any contaminants. The monomer was isolated after evaporation of the solvent under vacuum in a flask protected from direct exposure to light. Millipore water (18.2 M $\Omega$ ·cm) was added to yield a 1.29% weight/volume (w/v) suspension, which was sonicated at 65 °C for 30 min. The suspension was allowed to cool to room temperature, then stored at 4 °C overnight. The suspension was transferred to a crystallizing dish with a magnetic stir bar and irradiated with UV light (254 nm) for 8 min [33]. After the photo-polymerization, the dark blue suspension was transferred to a round bottom flask protected from light to remove the solvent under vacuum. The solid PDA was then stored at 4 °C and characterized by FT-IR. <sup>1</sup>H NMR (Proton nuclear magnetic resonance) characterization was not possible due to the impaired solubility of the material.

### **3.2.2. Electrospinning of PEO-PDA Fibers**

Mixture solutions of PEO and PCDA in chloroform were prepared at different mass ratios of PEO to PCDA (w/w %), different polymer (PEO and PCDA) concentrations, and different injection speed. Table 1 shows the experimental design for preparing PEO-PCDA fibers in the electrospinning.

Table 1 Electrospinning design for preparing Polyethylene oxide (PEO)-Pentacosadiynoic acid (PCDA) fibers.

<b>PEO:PCDA (w/w)</b>	<b>Polymer concentration (wt. %)</b>	<b>Injection speed (mL h<sup>-1</sup>)</b>	<b>Fiber identification (ID) number</b>
2:1	1.5	0.1	#1
		0.2	#2
	3.75	0.1	#3
		0.2	#4
	7.5	0.1	#5
		0.2	#6
3:1	1.33	0.1	#7
		0.2	#8
	3.34	0.1	#9
		0.2	#10
	6.67	0.1	#11
		0.2	#12
4:1	1.25	0.1	#13
		0.2	#14
	3.13	0.1	#15
		0.2	#16
	6.25	0.1	#17
		0.2	#18

The PEO and PCDA mixture solutions were stirred overnight on a hotplate stirrer at 350 revolutions per minute (rpm) at room temperature, resulting in a uniform light-pink solution. A customized electrospinning apparatus was used to prepare fibers. The apparatus primarily consisted of a Gamma High Voltage Research ES50P power supply and a Harvard PHD 2000

syringe pump. The uniform PEO-PCDA solution was injected at 0.1 mL h<sup>-1</sup> (or 0.2 mL h<sup>-1</sup>) and 15 KV. The spinning time was kept constant at 1 hour, resulting in a thick, colorless fiber mat. The fibers were collected at a distance of 17 cm on a collector plate. The obtained fibers were kept in the dark overnight before UV-light (Spectroline, Longlife<sup>TM</sup> filter, New York, USA) irradiation. During the irradiation with UV-light at 254 nm, the fibers became blue within 30 seconds and then turned deep blue in 3 minutes.

### **3.2.3. Fiber Characterization**

Fiber size and morphology was studied using scanning electron microscope (JEOL, JSM 6500F, Tokyo, Japan). The fiber samples were kept overnight under vacuum to evaporate any residual solvent or moisture. Then they were sputter-coated with gold to improve conductivity of the samples for better quality imaging. FTIR-attenuated total reflectance (ATR) spectra of PDA powders and PEO-PDA fibers were recorded in the range of 650–4000 cm<sup>-1</sup> using a Nicolet 6700 FTIR spectrometer (Thermo Electron Corporation, Madison, WI, USA). All materials were dried in a vacuum oven overnight at room temperature prior to the analysis. Two spectra were collected for each of the PDA-containing materials, one per color phase. In Figure 6, spectrum A represents the fibers during the blue phase, and B shows resonance features that correspond to the red fibers. The color change was induced by heating the blue fibers at 120 °C for 10 min to obtain red fibers. In addition, spectrum C depicts resonance features of the blue phase of PDAs, and spectrum D corresponds to the red phase of PDAs, where the color change was induced in the same manner as the fibers.

Differential scanning calorimetry (TA Q20 DSC) was used to determine the thermal transitions of the PEO-PDA fibers. The transitions were measured through three heating cycles under nitrogen flow. During the first heating cycle, the temperature was equilibrated at 40 °C and

ramped at 10 °C/min to 250 °C and equilibrated at 250 °C. In the second cycle, the temperature was ramped at 10 °C/min to -60 °C and equilibrated at -60 °C. For the third and final cycle, the temperature was ramped at 10 °C/min to 250 °C and equilibrated at 250 °C. Thermolyne benchtop furnace (Thermolyne, Thermo Fisher Scientific, Waltham, MA, USA) was used for exposing the fibers total treatment temperatures up to 120 °C.

#### **3.2.4. Colorimetric Transition of the PEO-PDA Fibers Due to Temperature Change**

The color of PEO-PDA fibers was measured using a spectrophotometer (HunterLab ColorQuest XE). Colorimetric transition behavior of the fibers was evaluated as a function of treatment temperature (25 °C, 50 °C, 60 °C, 70 °C, 80 °C, 90 °C, 100 °C, 110 °C, and 120 °C). Electrospun fiber mat samples (1 inch X 1 inch) were first treated in the benchtop furnace for 10 minutes at 25 °C. The fiber mat was then measured in the spectrophotometer and reflectance spectra were collected from 400 nm to 700 nm. The same fiber mat was later stored back to the furnace and treated at a higher temperature for another 10 minutes, following by reflectance measurement of the fiber mat. Reflectance spectra was collected for the same fiber mat after each heat treatment from 25 °C to 120 °C. For a given fiber mat treated at a given temperature, three spectrophotometric measurements were taken and the average reflectance was used for color analysis.

#### **4. Conclusions**

A mixture solution of PEO and PCDA was used to prepare PEO-PDA fibers via electrospinning. The PCDA self-assembled in the PEO matrix when the mixture solution was ejected in the electrospinning. The self-assembled PCDA were photo-polymerized upon UV light irradiation on the electrospun fibers. The size and surface roughness of the fibers was reduced when the mass ratio of PEO to PCDA was increased. A colorimetric change from blue

to red was observed when the fibers were treated at a temperature that was higher than 60 °C. The fibers obtained at a mass ratio of PEO to PCDA of 2:1 exhibited pronounced color switch behaviors at 70 °C. No further colorimetric change was found after the temperature was more than 110 °C. High sensitivity of color switch was also associated with low mass ratio of PEO to PCDA in the fibers as well as large size of the fibers. The FTIR and DSC analysis indicated that the color transition was due to a conformational change in PDA macromolecules. The results suggest that the PDA can be embedded into fibers capable of detecting a temperature that is more than 60 °C and signaling this change via a colorimetric change. It is significant that the PDA fiber composite does not change color at normal body temperature (35–37 °C) because this is able to exclude a false positive signal for biological sensing application, such as bacterial infection. No delay or retardation in color switch was observed in the PEO-PDA fiber composite, suggesting that the addition of PEO had no negative impact on the optical properties of the PDA. The study of electrospinning demonstrated that PEO significantly enhanced the spinnability of the PDA. PEO-PDA fiber composites are more economical compared to 100% PDA fiber used in wound dressing, further confirming that it is viable to develop PEO-PDA fiber composites especially for flexible biosensor applications. The responsive behavior of PEO-PDA fiber composites to bacteria is currently undergoing investigation, which will provide more information on the feasibility of using PEO-PDA fiber composites in wound dressings for detecting bacterial infection.

**Acknowledgements:** This work was funded by Bioscience Discovery Evaluation Grant Program (BDEGP) of the state of Colorado. J.P.Y. thankfully acknowledges the National Science Foundation for their financial contribution through the Alliance for Graduate Education and the Professoriate Fellowship (#PO0000062901).

**Author Contributions:** Literature survey, Electrospinning, SEM imaging, Heat treatment and Color measurement were done by A K M Mashud Alam. FTIR and DSC were done by J. Pamela Yapor. All the authors contributed equally in experiment design, data analysis and writing the manuscript. Dr. Yan Vivian Li and Dr. Melissa M. Reynolds, as the academic advisor to the first and second author respectively, provided motivation, guidance, and all sort of support during the work.

**Conflicts of Interest:** The authors declare no conflict of interest. The funding sponsors had no role in the design of the study, the collection, analyses, or interpretation of data, the writing of the manuscript, and the decision to publish the results.

### **Abbreviations**

PCDA: 10, 12-pentacosadiynoic acid

PDA : polydiacetylene

PEO: poly(ethylene oxide)

UV: ultra-violet

SEM: Scanning electron microscope

DSC: Differential scanning calorimeter

FTIR: Fourier transmission infrared radiation spectroscopy

VOC: volatile organic compound

PPM: parts per million

PMMA: polymethyl methacrylate

TEOS: tetraethyl orthosilicate

PS: polystyrene

## REFERENCES

- D'souza, S. Microbial biosensors. *Biosens. Bioelectron.* 2001, *16*, 337–353.
- Radke, S.M.; Alcocilja, E.C. A high density microelectrode array biosensor for detection of *E. Coli* O157: H7. *Biosens. Bioelectron.* 2005, *20*, 1662–1667.
- Thusu, R. Strong growth predicted for biosensors market. *Sensors* 2010.
- Dargaville, T.R.; Farrugia, B.L.; Broadbent, J.A.; Pace, S.; Upton, Z.; Voelcker, N.H. Sensors and imaging for wound healing: A review. *Biosens. Bioelectron.* 2013, *41*, 30–42.
- Velusamy, V.; Arshak, K.; Korostynska, O.; Oliwa, K.; Adley, C. An overview of foodborne pathogen detection: In the perspective of biosensors. *Biotech. Adv.* 2010, *28*, 232–254.
- Mandal, P.; Biswas, A.; Choi, K.; Pal, U. Methods for rapid detection of foodborne pathogens: An overview. *Am. J. Food Technol.* 2011, *6*, 87–102.
- Jelinek, R.; Ritenberg, M. Polydiacetylenes—recent molecular advances and applications. *RSC Adv.* 2013, *3*, 21192–21201.
- Sun, X.; Chen, T.; Huang, S.; Li, L.; Peng, H. Chromatic polydiacetylene with novel sensitivity. *Chem. Soc. Rev.* 2010, *39*, 4244–4257.
- Wu, A.; Beck, C.; Ying, Y.; Federici, J.; Iqbal, Z. Thermochromism in polydiacetylene–ZnO nanocomposites. *J. Phys. Chem.* 2013, *117*, 19593–19600.
- Pindzola, B.A.; Nguyen, A.T.; Reppy, M.A. Antibody-functionalized polydiacetylene coatings on nanoporous membranes for microorganism detection. *Chem. Commun.* 2006, *8*, 906–908.

- Kolusheva, S.; Kafri, R.; Katz, M.; Jelinek, R. Rapid colorimetric detection of antibody-epitope recognition at a biomimetic membrane interface. *J. Am. Chem. Soc.* 2001, *123*, 417–422.
- Charych, D.H.; Nagy, J.O.; Spevak, W.; Bednarski, M.D. Direct colorimetric detection of a receptor-ligand interaction by a polymerized bilayer assembly. *Science* 1993, *261*, 585–588.
- Kim, J.-M.; Lee, J.-S.; Choi, H.; Sohn, D.; Ahn, D.J. Rational design and in-situ FTIR analyses of colorimetrically reversible polydiacetylene supramolecules. *Macromolecules* 2005, *38*, 9366–9376.
- Lee, J.; Yarimaga, O.; Lee, C.H.; Choi, Y.K.; Kim, J.M. Network polydiacetylene films: Preparation, patterning, and sensor applications. *Adv. Funct. Mater.* 2011, *21*, 1032–1039.
- Mino, N.; Tamura, H.; Ogawa, K. Analysis of color transitions and changes on langmuir-blodgett films of a polydiacetylene derivative. *Langmuir* 1991, *7*, 2336–2341.
- Chance, R.; Baughman, R.; Müller, H.; Eckhardt, C.J. Thermochromism in a polydiacetylene crystal. *J. Chem. Phys.* 1977, *67*, 3616–3618.
- Chae, S.K.; Park, H.; Yoon, J.; Lee, C.H.; Ahn, D.J.; Kim, J.M. Polydiacetylene supramolecules in electrospun microfibers: Fabrication, micropatterning, and sensor applications. *Adv. Mater.* 2007, *19*, 521.
- Yoon, J.; Kim, J.M. Fabrication of conjugated polymer supramolecules in electrospun micro/nanofibers. *Macromol. Chem. Phys.* 2008, *209*, 2194–2203.
- Wu, J.; Lu, X.; Shan, F.; Guan, J.; Lu, Q. Polydiacetylene-embedded supramolecular electrospun fibres for a colourimetric sensor of organic amine vapour. *RSC Adv.* 2013, *3*, 22841–22844.

- Jeon, H.; Lee, J.; Kim, M.H.; Yoon, J. Polydiacetylene-based electrospun fibers for detection of HCl gas. *Macromol. Rapid Commun.* 2012, *33*, 972–976.
- Steyaert, I.; Rahier, H.; De Clerck, K. Nanofibre-based sensors for visual and optical monitoring. In *Electrospinning for high performance sensors*; Springer: New York, NY, USA, 2015; pp. 157–177.
- Yoon, J.; Chae, S.K.; Kim, J.M. Colorimetric sensors for volatile organic compounds (VOCs) based on conjugated polymer-embedded electrospun fibers. *J. Am. Chem. Soc.* 2007, *129*, 3038–3039.
- Shenoy, S.L.; Bates, W.D.; Frisch, H.L.; Wnek, G.E. Role of chain entanglements on fiber formation during electrospinning of polymer solutions: Good solvent, non-specific polymer–polymer interaction limit. *Polymer* 2005, *46*, 3372–3384.
- Edwards-Jones, V., Ed.; *Essential Microbiology for Wound Care*, 1st ed.; Oxford University Press: Oxford, UK, 2016.
- McKee, M.G.; Wilkes, G.L.; Colby, R.H.; Long, T.E. Correlations of solution rheology with electrospun fiber formation of linear and branched polyesters. *Macromolecules* 2004, *37*, 1760–1767.
- Nie, H.; He, A.; Wu, W.; Zheng, J.; Xu, S.; Li, J.; Han, C.C. Effect of poly (ethylene oxide) with different molecular weights on the electrospinnability of sodium alginate. *Polymer* 2009, *50*, 4926–4934.

- Sharma, S.; Khawaja, M.; Ram, M.K.; Goswami, D.Y.; Stefanakos, E. Characterization of 10,12-pentacosadiynoic acid langmuir–blodgett monolayers and their use in metal–insulator–metal tunnel devices. *Beilstein J. Nanotechnol.* 2014, 5, 2240–2247.
- Sukwattanasinitt, M.; Lee, D.C.; Kim, M.; Wang, X.; Li, L.; Yang, K.; Kumar, J.; Tripathy, S.K.; Sandman, D.J. New processable, functionalizable polydiacetylenes. *Macromolecules* 1999, 32, 7361–7369.
- Scoville, S.; Shirley, W. Investigations of chromatic transformations of polydiacetylene with aromatic compounds. *J. Appl. Polym. Sci.* 2011, 120, 2809–2820.
- Ahn, D.J.; Chae, E.H.; Lee, G.S.; Shim, H.Y.; Chang, T.E.; Ahn, K.D.; Kim, J.M. Colorimetric reversibility of polydiacetylene supramolecules having enhanced hydrogen-bonding under thermal and ph stimuli. *J. Am. Chem. Soc.* 2003, 125, 8976–8977.
- Luongo, J. Infrared study of oxygenated groups formed in polyethylene during oxidation. *J. Polym. Sci.* 1960, 42, 139–150.
- Chance, R.; Patel, G.; Witt, J. Thermal effects on the optical properties of single crystals and solution-cast films of urethane substituted polydiacetylenes. *J. Chem. Phys.* 1979, 71, 206–211.
- Champaiboon, T.; Tumcharern, G.; Potisatityuenyong, A.; Wacharasindhu, S.; Sukwattanasinitt, M. A polydiacetylene multilayer film for naked eye detection of aromatic compounds. *Sensor Actuat. B-Chem.* 2009, 139, 532–537.

## CHAPTER 5. CONCLUSIONS

A spinning solution containing PEO and PCDA was used to prepare PEO-PDA fibers via an electrospinning technique. When the mixture solution was ejected in the electrospinning, the solvent evaporated, and the PCDA self-assembled in the PEO matrix. The self-assembled PCDA were then photo-polymerized upon UV-light irradiation of the electrospun fiber mats. Finer fibers were obtained at low concentrations, low injection speed and higher mass ratio of PEO to PCDA. Continuous fibers without beads were favored at concentrations over 3.0 (w/w) %, below which beaded fibers were obtained. Smoother surfaces were obtained for the fibers with larger diameter.

When the fibers were treated at a temperature higher than 60 °C, the fiber mats exhibited a color transition from blue to red. High sensitivity of color switch was associated with low mass ratio of PEO to PCDA in the fibers as well as large size of the fibers. The fiber mats that were obtained at a mass ratio of 2:1 of PEO to PCDA exhibited a more pronounced color switch at 70 °C than the fibers prepared at mass ratios of 3:1 and 4:1. The color transition continued until the temperature was raised to 110 °C. No further colorimetric change was observed after the temperature was higher than 110 °C. The DSC analysis shows that the melting temperature falls in the range of 60–70 °C where the occurrence of color transition from blue to red was observed in the fibers. The similarities of the blue and red phase PDAs on the FT-IR spectra confirm that the PDAs retain its functional groups as it transitions from blue to red. However, changes in absorption wavelengths suggest a strain due to rotation in the conjugated backbone of the PDAs upon high temperature. This strain reduces the conjugation length and cause changes in electronic configuration of macromolecular structures of PDAs, which is manifested *via* a color

switch from blue to red. The consistency among the ColorQuest, FT-IR, and DSC data indicated that the color transition was due to a conformational change in PDA macromolecules. It is significant that the PDA fiber composite does not change color at normal body temperature (35–37 °C), and hence this is able to exclude a false positive signal for biological sensing application, such as bacterial infection. No delay or retardation in color switch was observed in the PEO-PDA fiber composite, suggesting that the addition of PEO had no negative impact on the optical properties of the PDA. The study demonstrated that the spinnability of the PDA fiber composites was significantly enhanced by the addition of PEO. PEO-PDA fiber composites are more economical compared to 100% PDA fiber used in wound dressing, further confirming that it is feasible to develop PEO-PDA fiber composites especially for flexible biosensor applications.

The development of PEO-PDA fiber composites for wound dressing biosensor, and their colorimetric transitional properties as a function of temperature was studied. Further investigation is suggested as follows:

1. An investigation on the color change of PEO-PDA fiber composites to the biomolecules, such as *E. coli* and *Staphylococcus aureus* can be conducted. The sensitivity and selectivity of the color change can be evaluated.
2. The interaction between PDA and a matrix polymer such as PEO can be studied using atomic force microscopy.
3. Further research could be conducted on the development of PDA fiber composites with other matrix polymers including poly(methyl methacrylate) (PMMA), polyurethane (PU), and cellulose acetate (CA). The colorimetric transition properties of the PDA fiber composites responding to temperature, bacteria, pH can be studied and compared with different polymer composites.

4. The mechanical properties of the PDA composites with various matrix polymer can be compared to evaluate the suitability of the fiber composite to be incorporate into an in-vivo wound dressing biosensor.

## REFERENCES

- Ahn, D. J., Chae, E. H., Lee, G. S., Shim, H. Y., Chang, T. E., Ahn, K. D., & Kim, J. M. (2003). Colorimetric reversibility of polydiacetylene supramolecules having enhanced hydrogen-bonding under thermal and pH stimuli. *Journal of the American Chemical Society*, *125*(30), 8976-8977.
- Ahn, D. J., & Kim, J. M. (2008). Fluorogenic polydiacetylene supramolecules: Immobilization, micropatterning, and application to label-free chemosensors. *Accounts of Chemical Research*, *41*(7), 805-816. DOI: 10.1021/ar7002489
- Bhardwaj, N., & Kundu, S. C. (2010). Electrospinning: A fascinating fiber fabrication technique. *Biotechnology Advances*, *28*(3), 325-347. DOI: 10.1016/j.biotechadv.2010.01.004
- Bhattacharai, N., Edmondson, D., Veisoh, O., Matsen, F. A., & Zhang, M. (2005). Electrospun chitosan-based nanofibers and their cellular compatibility. *Biomaterials*, *26*(31), 6176-6184. doi:10.1016/j.biomaterials.2005.03.027
- Buchko, C.J., Chen, L.C., Shen, Y., & Martin, D.C. (1999). Processing and microstructural characterization of porous biocompatible protein polymer thin films. *Polymer*, *40*(26), 7397-7407. DOI: 10.1016/S0032-3861(98)00866-0
- Casper, C.L., Stephens, J.S., Tassi, N.G., Chase, D.B., & Rabolt, J.F. (2004). Controlling surface morphology of electrospun polystyrene fibers: Effect of humidity and molecular weight in the electrospinning process. *Macromolecules*, *37*(2), 573-578. DOI: 10.1021/ma0351975

- Çete, S., & Bal, Ö. (2013). Preparation of Pt/polypyrrole–para toluene sulfonate hydrogen peroxide sensitive electrode for the utilizing as a biosensor. *Artificial cells, nanomedicine, and biotechnology*, 41(6), 414-420. DOI:10.3109/21691401.2012.759121
- Chae, S. K., Park, H., Yoon, J., Lee, C. H., Ahn, D. J., & Kim, J. M. (2007). Polydiacetylene supramolecules in electrospun microfibers: Fabrication, micropatterning, and sensor applications. *Advanced Materials*, 19(4), 521–524. DOI: 10.1002/adma.200602012
- Champaiboon, T., Tumcharern, G., Potisatityuenyong, A., Wacharasindhu, S., & Sukwattanasinitt, M. (2009). A polydiacetylene multilayer film for naked eye detection of aromatic compounds. *Sensors and Actuators B: Chemical*, 139(2), 532-537.
- Chance, R. R., Baughman, R. H., Müller, H., & Eckhardt, C. J. (1977). Thermo-chromism in a polydiacetylene crystal. *The Journal of Chemical Physics*, 67(8), 3616-3618.
- Chance, R. R., Patel, G. N., & Witt, J. D. (1979). Thermal effects on the optical properties of single crystals and solution-cast films of urethane substituted polydiacetylenes. *The Journal of Chemical Physics*, 71(1), 206-211.
- Charych, D.H., Nagy, J.O., Spevak, W., & Bednarski, M.D. (1993). Direct colorimetric detection of a receptor-ligand interaction by a polymerized bilayer assembly. *Science*, 261(5121), 585-588. DOI: 10.1126/science.8342021
- Chen, X., Zhou, G., Peng, X., & Yoon, J. (2012). Biosensors and chemosensors based on the optical responses of polydiacetylenes. *Chemical Society Review*, 41(13), 4610–4630. DOI: 10.1039/C2CS35055F

- Clarke, S. F., & Foster, J. R. (2012). A history of blood glucose meters and their role in self-monitoring of diabetes mellitus. *British Journal of Biomedical Science*, *69*(2), 83-93.
- Dargaville, T. R., Farrugia, B. L., Broadbent, J. A., Pace, S., Upton, Z., & Voelcker, N. H. (2013, March 15). Sensors and imaging for wound healing : A review. *Biosensors and Bioelectronics*, *41*(1), 30-42. doi:doi:10.1016/j.bios.2012.09.029
- Demir, M.M., Yilgor, I., Yilgor, E., & Erman, B. (2002). Electrospinning of polyurethane fibers. *Polymer*, *43*(11), 3303–3339. DOI: 10.1016/S0032-3861(02)00136-2
- D'souza, S. F. (2001). Microbial biosensors. *Biosensors and Bioelectronics*, *16*(6), 337-353.
- Edwards-Jones, V. (2016). *Essential Microbiology for Wound Care*. Oxford University Press, Oxford, UK.
- Geng, X., Kwon, O.H., & Jang, J. (2005). Electrospinning of chitosan dissolved in concentrated acetic acid solution. *Biomaterials*, *26*(27), 5427–5432. DOI: 10.1016/j.biomaterials.2005.01.066
- Gerard, M., Chaubey, A., & Malhotra, B. D. (2002). Application of conducting polymers to biosensors. *Biosensors and Bioelectronics*, *17*(5), 345-359. doi:10.1016/S0956-5663(01)00312-8
- Haghi, A.K., & Akbari, M. (2007). Trends in electrospinning of natural nanofibers. *Physica Status Solidi*, *204*(6), 1830–1834. doi: 10.1002/pssa.200675301

- Hill, E. H., Goswami, S., Evans, D. G., & Schanze, K. S. (2012). Photochemistry of a Model Cationic p-Phenylene Ethynylene in Water. *The Journal of Physical Chemistry*, 3(10), 1363-1368. doi:DOI: 10.1021/jz3004427
- Hohman, M.M., Shin, M., Rutledge, G., & Brenner, M.P. (2001). Electrospinning and electrically forced jets. II. Applications. *Physics of Fluids*, 13(8), 2221–2236. doi: 10.1063/1.1383791
- Jelinek, R., & Ritenberg, M. (2013). Polydiacetylenes—recent molecular advances and applications. *RSC Advances*,3(44), 21192-21201. DOI: 10.1039/c3ra42639d
- Jeon, H., Lee, J., Kim, M. H., & Yoon, J. (2012). Polydiacetylene-Based Electrospun Fibers for Detection of HCl Gas. *Macromolecular rapid communications*, 33(11), 972-976.
- Kim, J. M., Lee, J. S., Choi, H., Sohn, D., & Ahn, D. J. (2005). Rational design and in-situ FTIR analyses of colorimetrically reversible polydiacetylene supramolecules. *Macromolecules*, 38(22), 9366-9376.
- Koenen, J.-M., Zhu, X., Pan, Z., Feng, F., Yang, J., & Schanze, K. S. (2014). Enhanced fluorescence properties of Poly(phenylene ethynylene) conjugated polyelectrolytes designed to avoid aggregation. *ACS Macro Letters*, 3(5), 405-409. doi:DOI: 10.1021/mz500067k
- Kolusheva, S., Kafri, R., Katz, M., & Jelinek, R. (2001). Rapid colorimetric detection of antibody-epitope recognition at a biomimetic membrane interface. *Journal of the American Chemical Society*, 123(3), 417-422. doi:10.1021/ja0034139

- Larrondo, L., & Manley, R.S.J. (1981). Electrostatic fiber spinning from polymer melts. II. Examination of the flow field in an electrically driven jet. *Journal of Polymer Science: Polymer Physics*, 19(6), 921–932. DOI: 10.1002/pol.1981.180190602
- Lebouch, N., Garreau, S., Louarn, G., Belletête, M., Durocher, G., Lecle, M., & Whitten, D. G. (2005). Structural Study of the Thermochromic Transition in Poly(2,5-dialkyl-p-phenyleneethynylene)s. *Macromolecules*, 38(23), 9631–9637. doi:10.1021/ma051342y
- Lee, J., Pyo, M., Lee, S. H., Kim, J., Ra, M., Kim, W. Y., Park, B.J., Lee, C. W., & Kim, J.M. (2014). Hydrochromic conjugated polymers for human sweat pore mapping. *Nature Communications*, 5(1), 1-10. DOI: 10.1038/ncomms4736
- Lee, J., Yarimaga, O., Lee, C.H., Choi, Y.K., & Kim, J.M. (2011). Network polydiacetylene films: Preparation, patterning and sensor applications. *Advanced Functional Materials*, 21(6), 1032-1039. DOI:10.2012/adfm.201002042
- Lee, K., Povlich, L.K., & Kim, J. (2010). Recent advances in fluorescent and colorimetric conjugated polymer-based biosensors. *Analyst*, 135(9), 2179-2189. DOI: 10.1039/C0AN00239A
- Li, D., & Xia, Y. (2004). Electrospinning of nanofibers: Reinventing the wheel? *Advance Materials*, 16(14), 1151–1170. doi: 10.1002/adma.200400719
- Liang, D., Hsiao, B.S., & Chu, B. (2007). Functional electrospun nanofibrous scaffolds for biomedical applications. *Advanced Drug Delivery Reviews*, 59(14), 1392–1412. DOI: 10.1016/j.addr.2007.04.021

- Li, P., Zhang, B., & Cui, T. (2015). Towards intrinsic graphene biosensor: A label-free, suspended single crystalline graphene sensor for multiplex lung cancer tumor markers detection. *Biosensors and Bioelectronics*, 72, 168-174. doi:10.1016/j.bios.2015.05.007
- Luongo, J. P. (1960). Infrared study of oxygenated groups formed in polyethylene during oxidation. *Journal of Polymer Science*, 42(139), 139-150.
- Mandal, P. K., Biswas, A. K., Choi, K., & Pal, U. K. (2011). Methods for rapid detection of foodborne pathogens: An overview. *American Journal of Food Technology*, 6(2), 87-102. doi: 10.3923/ajft.2011.87.102
- Marsella, M. J., & Swager, T. M. (1993). Designing conducting polymer-based sensors: selective ionochromic response in crown ether-containing polythiophenes. *Journal of the American Chemical Society*, 115(25), 12214-12215. DOI: 10.1021/ja00078a090
- Mckee, M.G., Wilkes, G.L., Colby, R.H., & Long, T.E. (2004). Correlations of solution rheology with electrospun fiber formation of linear and branched polyesters. *Macromolecules*, 37(5), 1760–1767. DOI: 10.1021/ma035689h
- Mino, N., Tamura, H., & Ogawa, K. (1991). Analysis of color transitions and changes on Langmuir-Blodgett films of a polydiacetylene derivative. *Langmuir*, 7(10), 2336-2341.
- Mit-uppatham, C., Nithitanakul, M., & Supaphol, P. (2004). Ultrafine electrospun polyamide-6 fibers: effect of solution conditions on morphology and average fiber diameter. *Macromolecular Chemistry and Physics*, 205(17), 2327–2738. DOI: 10.1002/macp.200400225

- Nandana, B., & Kundu, S. C. (2010). Electrospinning: A fascinating fiber fabrication technique. *Biotechnology Advances*, 28(3), 325–347. DOI: 10.1016/j.biotechadv.2010.01.004
- Nie, H., He, A., Wu, W., Zheng, J., Xu, S., Li, J., & Han, C. C. (2009). Effect of poly (ethylene oxide) with different molecular weights on the electrospinnability of sodium alginate. *Polymer*, 50(20), 4926-4934.
- Oliveiraa, T. d., Soaresa, N. d., Silva, D. J., Andrade, N. d., & Medeiros, E. A. (2013). Development of PDA/Phospholipids/Lysine vesicles to detect pathogenic bacteria. *Sensors and Actuators B: Chemical*, 188, 385-392. doi:10.1016/j.snb.2013.06.022
- Pham, Q.P., Sharma, U., & Mikos, A.G. (2006). Electrospinning of polymeric nanofibers for tissue engineering applications. *Tissue Engineering*, 12(5), 1197-1211. doi:10.1089/ten.2006.12.1197.
- Pindzola, B. A.; Nguyen, A. T.; & Reppy, M. A. (2006). Antibody-functionalized polydiacetylene coatings on nanoporous membranes for microorganism detection. *Chemical Communications*, 8, 906-908. doi: 10.1039/B516403F
- Pun, C. C., Lee, K., Kim, H. J., & Kim, J. (2006). Signal amplifying conjugated polymer-based solid-state DNA sensors. *Macromolecules*, 39(22), 7461-7463. doi: 10.1021/ma061330s
- Radke, S. M., & Alocilja, E. C. (2005). A high density microelectrode array biosensor for detection of E. coli O157: H7. *Biosensors and Bioelectronics*, 20(8), 1662-1667.
- Reneker, D. H., & Chun, I. (1996). Nanometre diameter fibres of polymer, produced by electrospinning. *Nanotechnology*, 7(3), 216-223. doi:10.1088/0957-4484/7/3/009

- Sarkar, A. K., & Seal, C. M. (2003). Color strength and colorfastness of flax fabrics dyed with natural colorants. *Clothing and Textiles Research Journal*, 21(4), 162-166.
- Scoville, S. P., & Shirley, W. M. (2011). Investigations of chromatic transformations of polydiacetylene with aromatic compounds. *Journal of applied polymer science*, 120(5), 2809-2820.
- Sharma, S., Khawaja, M., Ram, M. K., Goswami, D. Y., & Stefanakos, E. (2014). Characterization of 10, 12-pentacosadiynoic acid Langmuir–Blodgett monolayers and their use in metal–insulator–metal tunnel devices. *Beilstein journal of nanotechnology*, 5(1), 2240-2247.
- Shenoy, S. L., Bates, W. D., Frisch, H. L., & Wnek, G. E. (2005). Role of chain entanglements on fiber formation during electrospinning of polymer solutions: good solvent, non-specific polymer–polymer interaction limit. *Polymer*, 46(10), 3372-3384.
- Steyaert, I., Rahier, H., & De Clerck, K. (2015). Nanofibre-Based Sensors for Visual and Optical Monitoring. In *Electrospinning for High Performance Sensors*. Springer International Publishing. p. 158.
- Sukwattanasinitt, M., Lee, D. C., Kim, M., Wang, X., Li, L., Yang, K., ... & Sandman, D. J. (1999). New processable, functionalizable polydiacetylenes. *Macromolecules*, 32(22), 7361-7369.
- Sun, X., Chen, T., Huang, S., Li, L., & Peng, H. (2010). Chromatic polydiacetylene with novel sensitivity. *Chemical Society Reviews*, 39(11), 4244-4257. DOI: 10.1039/C001151G

- Thusu, R. (2010, October 1). Strong Growth Predicted for Biosensors Market. Retrieved September 01, 2015, from <http://www.sensorsmag.com/specialty-markets/medical/strong-growth-predicted-biosensors-market-7640>
- Tan, C., Atas, E., Müller, J. G., Pinto, M. R., Kleiman, V. D., & Schanze, K. S. (2004). Amplified quenching of a conjugated polyelectrolyte by cyanine dyes. *Journal of the American Chemical Society*, *126*(42), 13685-13694. DOI: 10.1021/ja046856b
- Velusamy, V., Arshak, K., Korostynska, O., Oliwa, K., & Adley, C. (2010). An overview of foodborne pathogen detection: In the perspective of biosensors. *Biotechnology Advances*, *28*(2), 232-254. doi: 10.1016/j.biotechadv.2009.12.004
- Wang, M., Wang, F., Wang, Y., Zhang, W., & Chen, X. (2015). Polydiacetylene-based sensor for highly sensitive and selective Pb<sup>2+</sup> detection. *Dyes and Pigments*, *120*, 307-313. doi:10.1016/j.dyepig.2015.04.035
- Weatherall, I. L., & Coombs, B. D. (1992). Skin color measurements in terms of CIELAB color space values. *Journal of investigative dermatology*, *99*(4), 468-473.
- Wenz, G., Mueller, M. A., Schmidt, M., Wegner, G. (1984). Structure of poly(diacetylenes) in solution. *Macromolecules* 1984, *17* (4), 837-850. DOI: 10.1021/ma00134a052
- Wu, A., Beck, C., Ying, Y., Federici, J., & Iqbal, Z. (2013). Thermochromism in polydiacetylene–ZnO nanocomposites. *The Journal of Physical Chemistry C*, *117*(38), 19593-19600.

- Wu, J., Lu, X., Shan, F., Guan, J., & Lu, Q. (2013). Polydiacetylene-embedded supramolecular electrospun fibres for a colourimetric sensor of organic amine vapour. *RSC Advances*, 3(45), 22841-22844.
- Wu, L., Chu, H., Koh, W., & Li, E. (2010). Highly sensitive graphene biosensors based on surface plasmon resonance. *Optics Express*, 18(4), 14395-14400. doi: 10.1364/OE.18.014395
- Yoon, B., Lee, S., & Kim, J.M. (2009). Recent conceptual and technological advances in polydiacetylene-based supramolecular chemosensors. *Chemical Society Reviews*, 38(7), 1958-1968. DOI: 10.1039/B819539K
- Yoon, J., Chae, S. K., & Kim, J. M. (2007). Colorimetric sensors for volatile organic compounds (VOCs) based on conjugated polymer-embedded electrospun fibers. *Journal of the American Chemical Society*, 129(11), 3038-3039. DOI: 10.1021/ja067856
- Yoon, J., & Kim, J. M. (2008). Fabrication of conjugated polymer supramolecules in electrospun micro/nanofibers. *Macromolecular Chemistry and Physics*, 209(21), 2194-2203.
- Yoshida, K., Yoshioka, D., Inoue, K., Takaichi, S., & Maeda, I. (2007). Evaluation of colors in green mutants isolated from purple bacteria as a host for colorimetric whole-cell biosensors. *Applied Microbiology and Biotechnology*, 76(5), 1043-1050. doi:10.1007/s00253-007-1079-5
- Yuan, X.Y., Zhang, Y.Y., Dong, C.H., & Sheng J. (2004). Morphology of ultrafine Polysulfone fibers prepared by electrospinning. *Polymer International*, 53(11), 1704–1710.  
DOI:10.1002/pi.1538

Zhang, C., Yuan, X., Wu, L., Han, Y., & Sheng, J. (2005). Study on morphology of electrospun poly (vinyl alcohol) mats. *European Polymer Journal*, 41(3), 423–432. DOI: 10.1016/j.eurpolymj.2004.10.027

## APPENDICES

### Appendix 1: Fiber diameter distribution of the prepared samples

Table 2. Average diameter of the electrospun PEO-PDA fibers.

Mass Ratio, PEO: PCDA	Polymer Concentration%	Inj. Speed (ml hr <sup>-1</sup> )	Fiber ID #	Average Fiber Diameter (μm)	Standard Deviation
2:01	1.5	0.1	1	0.5	0.062
		0.2	2	0.64	0.062
	3.75	0.1	3	1.3	0.035
		0.2	4	1.7	0.177
	7.5	0.1	5	2.2	0.111
		0.2	6	3.4	0.062
3:01	1.33	0.1	7	0.38	0.043
		0.2	8	0.58	0.063
	3.34	0.1	9	1.3	0.104
		0.2	10	1.5	0.068
	6.67	0.1	11	1.3	0.058
		0.2	12	1.9	0.128
4:01	1.25	0.1	13	0.22	0.040
		0.2	14	0.52	0.053
	3.13	0.1	15	1.1	0.049
		0.2	16	1.6	0.058
	6.25	0.1	17	1.7	0.069
		0.2	18	1.9	0.052

**Appendix 2: Reflectance values for fiber composites prepared at 2:1 PEO: PCDA**

Table 3. Spectral reflectance data of the fiber composite (# 1) prepared at 2:1 PEO: PCDA, 1.5 w/w % concentration, and 0.1 ml hr<sup>-1</sup> injection speed.

Wavelength (nm)	Treatment Temperature								
	25 °C	50 °C	60 °C	70 °C	80 °C	90 °C	100 °C	110 °C	120 °C
400	45.64	41.96	40.55	38.9	39.62	40.88	41.69	41.84	42.71
410	44.94	40.97	39.66	37.94	38.83	40.19	40.76	40.89	41.9
420	43.31	39.4	37.73	35.95	36.93	38.35	39	39.15	40.11
430	42.01	37.81	35.75	33.84	34.98	36.49	37.28	37.49	38.54
440	41.04	36.58	34.28	32.21	33.48	35.08	35.97	36.15	37.21
450	39.61	35.03	32.39	30.32	31.79	33.52	34.61	34.77	35.82
460	38.34	33.67	30.91	28.96	30.67	32.57	33.71	33.86	34.89
470	37.18	32.32	29.5	27.69	29.66	31.76	32.95	33.1	34.15
480	36.37	31.18	28.59	26.99	29.16	31.39	32.7	32.78	33.85
490	34.33	29.68	26.99	25.67	28.04	30.39	31.69	31.82	32.82
500	33.06	28.49	26.4	25.38	27.86	30.3	31.54	31.66	32.68
510	31.86	27.41	26.35	25.71	28.19	30.59	31.87	31.99	33.00
520	30.85	26.44	26.35	26.17	28.68	31.08	32.4	32.55	33.66
530	29.43	25.45	25.61	25.79	28.26	30.73	32.11	32.32	33.51
540	28.31	25.02	25.35	25.7	27.91	30.43	31.79	31.96	33.11
550	27.27	24.84	26.05	26.65	28.41	30.83	31.97	32.06	33.04
560	26.9	24.82	27.98	29.76	31.49	33.88	34.35	34.39	35.04
570	26.31	24.45	28.48	32.42	35.9	42.06	45.88	46.01	46.37
580	25.86	24.14	28.58	33.67	38.29	47.68	56.64	57.01	57.09
590	25.86	24.14	28.76	34.28	39.42	50.93	65.67	66.38	66.36
600	25.97	24.29	28.97	34.61	39.93	52.43	70.32	71.18	71.26
610	25.72	24.09	28.73	34.58	40.03	53.02	71.76	72.6	72.75
620	25.01	23.32	28.01	34.07	39.69	53.09	72.48	73.21	73.32
630	24.45	22.89	27.34	33.38	39.19	53.05	73.04	73.67	73.78
640	24.54	23.09	27.42	33.25	39.08	53.26	73.35	73.9	73.99
650	25.28	24.05	28.56	34.22	39.9	54.26	73.79	74.23	74.33
660	28.21	27.2	31.18	36.1	41.47	56.08	73.36	73.8	73.95
670	34.81	33.95	36.62	40.19	44.79	59.52	73.14	73.63	73.75
680	45.62	44.99	45.6	47.76	51.56	65.04	73.22	73.72	73.84
690	56.97	56.25	56.26	57.8	60.61	69.57	73.33	73.74	73.78
700	64.63	63.33	63.67	64.6	66.76	71.61	72.8	73.17	73.44

Table 4. Spectral reflectance data of the fiber composite (# 2) prepared at 2:1 PEO: PCDA, 1.5 w/w % concentration, and 0.2 ml hr<sup>-1</sup> injection speed.

Wavelength (nm)	Treatment Temperature								
	25 °C	50 °C	60 °C	70 °C	80 °C	90 °C	100 °C	110 °C	120 °C
400	29.84	29.77	27.62	24.56	25.68	26.74	29.79	29.31	30.76
410	28.76	28.76	26.57	23.42	24.83	25.99	28.82	28.27	29.85
420	27.32	27.23	24.92	21.84	23.18	24.52	27.23	26.87	28.30
430	26.05	25.82	23.3	20.23	21.52	23.05	25.77	25.6	26.97
440	24.98	24.71	21.94	18.79	20.24	21.96	24.68	24.49	25.84
450	23.72	23.35	20.52	17.54	19.01	20.93	23.64	23.6	24.83
460	22.59	22.16	19.34	16.61	18.18	20.28	22.97	22.99	24.15
470	21.5	21.06	18.26	15.81	17.49	19.77	22.46	22.52	23.67
480	20.54	20.13	17.35	15.07	17.04	19.46	22.27	22.18	23.39
490	19.19	18.86	16.36	14.61	16.44	19.02	21.64	21.8	22.82
500	18.10	17.92	15.84	14.4	16.34	18.97	21.6	21.73	22.8
510	17.08	17.04	15.58	14.45	16.51	19.1	21.82	21.85	23.01
520	16.20	16.33	15.42	14.6	16.79	19.33	22.11	22.07	23.36
530	15.28	15.5	14.90	14.46	16.54	19.13	21.87	21.94	23.21
540	14.58	14.95	14.56	14.48	16.42	19.07	21.75	21.86	23.05
550	13.96	14.56	14.73	15.07	16.87	19.43	22.02	22.07	23.20
560	13.59	14.36	15.44	16.76	18.95	21.43	24.2	24.03	25.11
570	13.24	14.03	15.51	18.51	22.16	27.9	34.08	34.41	35.43
580	13.08	13.85	15.49	19.35	23.96	32.51	44.32	46.95	47.61
590	13.09	13.85	15.53	19.66	24.77	35.12	53.5	60.00	60.28
600	13.19	13.98	15.67	19.89	25.12	36.24	58.84	67.91	68.06
610	13.08	13.87	15.58	19.92	25.18	36.63	60.94	70.48	70.67
620	12.68	13.38	15.03	19.29	24.74	36.41	62.05	71.23	71.37
630	12.55	13.23	14.76	18.84	24.31	36.11	63.11	71.89	71.99
640	12.82	13.51	14.98	18.9	24.32	36.14	64.33	72.17	72.28
650	13.30	14.11	15.74	19.68	25.13	36.96	66.10	72.49	72.60
660	16.02	16.94	18.15	21.54	26.78	38.79	67.65	71.98	72.15
670	21.80	22.78	23.43	26.02	30.32	42.75	69.42	71.73	71.96
680	31.09	32.14	32.06	34.05	37.78	50.96	70.88	71.73	72.05
690	44.44	45.5	44.98	46.91	50.35	61.10	71.52	71.71	71.92
700	55.47	56.33	55.79	57.42	60.15	66.99	71.34	71.20	71.52

Table 5. Spectral reflectance data of the fiber composite (# 3) prepared at 2:1 PEO: PCDA, 3.75 w/w % concentration, and 0.1 ml hr<sup>-1</sup> injection speed.

Wavelength (nm)	Treatment Temperature								
	25 °C	50 °C	60 °C	70 °C	80 °C	90 °C	100 °C	110 °C	120 °C
400	24.82	24.62	22.29	20.26	21.67	22.2	23.71	23.20	23.26
410	23.69	23.52	21.15	19.16	20.57	21.06	22.27	21.83	21.94
420	22.21	21.99	19.6	17.5	18.78	19.24	20.24	19.95	20.03
430	20.98	20.53	18.05	15.86	17.07	17.50	18.44	18.23	18.31
440	19.94	19.45	16.9	14.75	15.97	16.38	17.18	17.08	17.15
450	18.81	18.23	15.72	13.77	14.98	15.40	16.19	16.13	16.19
460	17.81	17.23	14.79	13.15	14.40	14.85	15.57	15.57	15.61
470	16.89	16.27	13.95	12.66	13.98	14.46	15.16	15.18	15.23
480	16.07	15.50	13.27	12.42	13.80	14.32	15.05	15.13	15.18
490	15.06	14.61	12.63	12.14	13.55	14.12	14.80	14.91	14.95
500	14.23	13.92	12.26	12.22	13.71	14.29	14.99	15.11	15.20
510	13.45	13.32	12.05	12.44	13.95	14.50	15.25	15.38	15.54
520	12.79	12.78	11.88	12.67	14.17	14.67	15.45	15.60	15.81
530	12.15	12.20	11.48	12.57	14.00	14.52	15.28	15.41	15.64
540	11.71	11.85	11.28	12.67	14.12	14.69	15.42	15.52	15.70
550	11.33	11.63	11.42	13.18	14.54	15.04	15.81	15.89	16.10
560	11.08	11.47	11.75	16.14	18.02	18.48	19.34	19.46	19.89
570	10.82	11.18	11.60	25.15	29.81	30.97	32.76	33.09	33.88
580	10.74	11.07	11.53	33.40	43.11	45.57	49.27	49.89	50.92
590	10.76	11.07	11.54	38.71	53.23	56.72	62.50	63.32	64.31
600	10.85	11.19	11.73	41.30	58.05	61.90	68.73	69.55	70.50
610	10.86	11.25	11.81	42.06	59.58	63.50	70.42	71.19	72.16
620	10.56	10.86	11.3	40.84	59.89	63.86	70.99	71.78	72.77
630	10.53	10.74	11.04	39.26	60.12	64.23	71.50	72.21	73.25
640	10.72	10.89	11.13	38.98	60.63	64.65	71.71	72.34	73.33
650	10.65	10.99	11.4	41.56	62.08	65.65	72.04	72.6	73.63
660	12.83	13.5	14.19	47.35	63.68	66.39	71.46	72.11	73.14
670	19.80	21.27	22.3	55.4	65.57	67.33	71.01	71.89	73.01
680	33.39	36.15	37.58	62.94	67.61	68.58	70.98	71.98	73.20
690	51.27	53.89	55.39	67.12	69.18	69.65	71.23	71.90	73.15
700	62.90	65.09	66.39	68.78	69.47	70.02	71.10	71.52	72.72

Table 6. Spectral reflectance data of the fiber composite (# 4) prepared at 2:1 PEO: PCDA, 3.75 w/w % concentration, and 0.2 ml hr<sup>-1</sup> injection speed.

Wavelength (nm)	Treatment Temperature								
	25 °C	50 °C	60 °C	70 °C	80 °C	90 °C	100 °C	110 °C	120 °C
400	24.57	24.14	22.44	19.91	21.98	22.09	23	22.31	22.76
410	23.5	23.11	21.5	18.82	21	21.04	21.64	20.98	21.39
420	22.14	21.69	19.98	17.36	19.31	19.37	19.87	19.48	19.71
430	20.99	20.36	18.5	15.9	17.73	17.79	18.28	18.14	18.18
440	19.97	19.38	17.43	14.82	16.69	16.66	17.14	16.97	16.97
450	18.88	18.19	16.24	13.95	15.73	15.74	16.22	16.22	16.1
460	17.89	17.2	15.28	13.4	15.18	15.2	15.65	15.71	15.54
470	16.98	16.27	14.4	12.99	14.76	14.8	15.27	15.4	15.17
480	16.12	15.52	13.74	12.69	14.61	14.6	15.14	15.13	14.98
490	15.15	14.58	12.99	12.54	14.3	14.44	14.92	15.1	14.84
500	14.31	13.87	12.56	12.59	14.4	14.59	15.09	15.23	15.03
510	13.5	13.25	12.26	12.73	14.59	14.78	15.35	15.36	15.32
520	12.84	12.74	12.02	12.89	14.8	14.93	15.53	15.49	15.57
530	12.24	12.18	11.62	12.82	14.63	14.81	15.4	15.41	15.46
540	11.82	11.82	11.41	12.98	14.69	14.96	15.5	15.56	15.54
550	11.46	11.56	11.41	13.3	14.92	15.26	15.79	15.83	15.9
560	11.23	11.42	11.59	15.18	16.93	17.55	17.97	17.96	18.4
570	10.98	11.17	11.37	23.58	26.19	28.67	29.45	29.69	30.62
580	10.92	11.09	11.3	32.74	36.64	43.33	45.51	46	47.32
590	10.93	11.07	11.3	39.66	44.8	56.2	60.4	60.67	62.02
600	10.98	11.16	11.42	43.23	48.91	62.84	68.01	68.03	69.31
610	11.02	11.2	11.46	44.43	50.21	65.09	70.17	70.11	71.42
620	10.78	10.95	11.12	43.56	49.77	65.73	70.81	70.75	72.1
630	10.81	10.92	11.04	42.49	49.17	66.47	71.37	71.29	72.65
640	11	11.12	11.2	42.64	49.59	67.16	71.61	71.46	72.82
650	10.96	11.12	11.18	45.51	52.15	68.23	71.93	71.71	73.12
660	11.8	12.02	12.64	51.21	56.43	68.73	71.37	71.21	72.69
670	16.9	17.35	18.83	58.7	61.51	69.25	71.04	70.97	72.59
680	29.03	29.77	32.24	65.47	66.06	69.9	71.06	71.13	72.78
690	46.85	47.8	50.81	69.11	68.92	70.34	71.12	71.07	72.79
700	59.73	60.32	62.67	70.33	70.02	70.36	70.77	70.74	72.35

Table 7. Spectral reflectance data of the fiber composite (# 5) prepared at 2:1 PEO: PCDA, 7.5 w/w % concentration, and 0.1 ml hr<sup>-1</sup> injection speed.

Wavelength (nm)	Treatment Temperature								
	25 °C	50 °C	60 °C	70 °C	80 °C	90 °C	100 °C	110 °C	120 °C
400	34.88	36.07	32.53	34.04	34.64	36.31	39.14	37.10	38.25
410	33.63	34.99	31.19	33.06	33.63	35.32	37.83	35.92	37.02
420	32.00	33.14	29.19	31.00	31.74	33.19	35.59	33.8	34.85
430	30.59	31.26	27.26	29.12	29.97	31.25	33.51	31.85	32.90
440	29.32	30.12	25.63	27.75	28.63	29.82	31.92	30.41	31.39
450	27.88	28.44	24.03	26.32	27.35	28.37	30.39	29.00	29.90
460	26.55	27.12	22.73	25.39	26.52	27.46	29.35	28.05	28.90
470	25.28	25.80	21.57	24.66	25.88	26.78	28.53	27.32	28.14
480	24.03	25.05	20.61	24.37	25.53	26.52	28.25	27.14	27.88
490	22.50	23.45	19.73	23.52	24.89	25.69	27.34	26.25	26.99
500	21.11	22.44	19.31	23.57	24.89	25.77	27.35	26.29	27.01
510	19.73	21.6	19.19	23.91	25.13	26.11	27.76	26.71	27.46
520	18.49	20.8	19.09	24.37	25.47	26.55	28.32	27.29	28.14
530	17.35	19.79	18.58	24.1	25.14	26.18	27.99	26.98	27.87
540	16.46	19.09	18.47	24.05	24.97	25.97	27.66	26.63	27.43
550	15.62	18.53	19.27	24.71	25.31	26.31	27.93	26.78	27.53
560	15.01	18.31	20.91	28.42	29.05	30.4	32.39	31.19	32.44
570	14.53	17.76	21.28	39.97	41.82	44.22	46.97	45.74	47.63
580	14.24	17.36	21.25	49.42	53.47	57.38	60.48	59.59	61.49
590	14.12	17.26	21.14	55.37	61.34	66.58	69.7	69.35	70.70
600	14.23	17.44	21.44	58.09	64.82	70.6	73.54	73.51	74.52
610	14.33	17.48	21.74	58.87	65.85	71.78	74.41	74.47	75.40
620	13.74	16.74	20.64	58.21	65.87	72.12	74.75	74.89	75.79
630	13.29	16.06	19.5	57.16	65.9	72.46	74.99	75.18	76.04
640	13.20	15.82	18.92	57.03	66.28	72.67	74.97	75.15	76.01
650	13.14	16.11	19.42	59.23	67.72	73.14	75.17	75.41	76.20
660	15.77	19.53	23.42	63.26	69.22	73.07	74.62	74.84	75.67
670	24.04	28.86	33.13	67.98	70.75	73.00	74.26	74.56	75.44
680	40.06	45.79	50.36	71.8	72.23	73.32	74.26	74.66	75.57
690	57.89	61.67	64.78	73.33	73.11	73.55	74.23	74.66	75.46
700	68.53	70.71	72.48	74.05	73.21	73.43	73.85	74.08	75.02

Table 8. Spectral reflectance data of the fiber composite (# 6) prepared at 2:1 PEO: PCDA, 7.5 w/w % concentration, and 0.2 ml hr<sup>-1</sup> injection speed.

Wavelength (nm)	Treatment Temperature								
	25 °C	50 °C	60 °C	70 °C	80 °C	90 °C	100 °C	110 °C	120 °C
400	37.3	33.43	29.96	36.34	38.04	39.15	41.05	37.78	38.49
410	36.17	32.19	28.51	35.17	36.83	37.91	39.55	36.45	37.22
420	34.4	30.34	26.53	33.39	34.89	35.83	37.53	34.55	35.24
430	32.88	28.58	24.5	31.5	32.89	33.76	35.45	32.68	33.23
440	31.74	27.3	22.9	30.07	31.36	32.06	33.74	31.12	31.6
450	30.23	25.74	21.32	28.65	29.86	30.45	32.15	29.75	30.08
460	28.9	24.43	20.14	27.69	28.84	29.35	31	28.73	28.98
470	27.64	23.21	19	26.81	27.92	28.4	29.94	27.87	28.02
480	26.62	22.27	18.17	26.2	27.27	27.66	29.27	27.28	27.41
490	24.89	20.99	17.31	25.5	26.54	26.94	28.43	26.61	26.63
500	23.56	20.1	16.96	25.32	26.35	26.75	28.15	26.44	26.45
510	22.21	19.24	17.03	25.54	26.56	26.95	28.44	26.69	26.78
520	20.92	18.37	17.18	25.84	26.89	27.29	28.91	27.13	27.38
530	19.5	17.4	16.72	25.54	26.47	26.92	28.57	26.86	27.12
540	18.42	16.86	16.39	25.34	26.06	26.5	28	26.4	26.47
550	17.35	16.47	17.14	25.85	26.38	26.81	28.18	26.52	26.53
560	16.58	16.16	20.17	29.97	30.84	31.47	33.07	31.09	32.17
570	15.78	15.49	22.96	43.55	45.05	46.16	47.94	45.97	48.13
580	15.22	15.01	24.04	56.54	58.5	59.88	61.15	60.01	62.33
590	14.85	14.68	23.95	65.62	67.72	68.93	69.69	69.33	71.1
600	14.67	14.56	23.99	69.42	71.45	72.55	72.99	73.04	74.41
610	14.89	14.83	24.78	70.41	72.32	73.45	73.57	73.82	75.09
620	14.68	14.56	24.23	70.56	72.52	73.59	73.84	74.11	75.4
630	14	13.88	22.58	70.68	72.79	73.84	74.01	74.28	75.55
640	13.2	13.13	20.75	70.83	72.87	73.84	73.9	74.19	75.4
650	12.83	12.84	19.88	71.58	73.12	73.94	74.07	74.27	75.46
660	12.96	13.14	21.95	71.8	72.48	73.34	73.46	73.7	74.94
670	15.78	16.34	29.04	71.94	71.77	72.63	73.07	73.38	74.85
680	23.4	24.66	43.6	72.2	71.61	72.46	73.1	73.54	75.2
690	37.44	39.54	62.06	72.44	72.13	72.72	73.15	73.6	75.31
700	53.78	55.31	71.72	72.03	71.95	72.62	72.73	73.14	74.75

### Appendix 3: Reflectance values for fiber composites prepared at 3:1 PEO: PCDA

Table 9. Spectral reflectance data of the fiber composite (# 7) prepared at 3:1 PEO: PCDA, 1.33 w/w % concentration, and 0.1 ml hr<sup>-1</sup> injection speed.

Wavelength (nm)	Treatment Temperature								
	25 °C	50 °C	60 °C	70 °C	80 °C	90 °C	100 °C	110 °C	120 °C
400	50.43	50.35	50.48	47.8	50.16	54.14	55.42	55.77	55.97
410	49.32	49.09	48.88	46.15	48.69	52.52	54.2	54.19	54.74
420	47.77	47.4	47.17	44.52	46.66	50.19	51.78	52.43	52.30
430	46.41	45.92	45.56	42.85	44.66	47.85	49.6	50.39	50.10
440	45.04	44.45	43.57	40.69	42.46	45.6	47.64	48.46	48.12
450	43.58	42.9	42	39.19	40.68	43.63	45.62	46.72	46.08
460	42.11	41.39	40.39	37.8	39.18	42.02	44.07	45.3	44.51
470	40.75	40	38.91	36.51	37.81	40.53	42.7	43.94	43.13
480	39.26	38.55	37	34.88	36.46	39.22	41.88	42.71	42.30
490	37.31	36.72	35.87	34.21	35.33	37.99	40.16	41.77	40.56
500	35.51	35.15	34.73	33.69	34.97	37.59	39.92	41.13	40.32
510	33.62	33.51	33.76	33.88	35.36	38.09	40.6	41.8	41.01
520	31.89	31.97	32.73	34.16	35.95	38.82	41.65	43.09	42.07
530	30.11	30.32	31.49	33.7	35.37	38.29	41.16	43.51	41.57
540	28.59	29.01	30.61	33.17	34.7	37.53	40.32	42.55	40.72
550	27.12	27.8	30.56	34.56	36.06	38.83	41.15	42.45	41.56
560	26.02	26.88	30.75	39.82	42.38	45.66	47.15	48.47	47.62
570	25.21	26.1	30.52	46.71	53.19	59.33	60.29	62.62	60.89
580	24.6	25.49	30.12	50.2	59.53	68.09	69.43	71.77	70.12
590	24.48	25.39	29.97	51.44	62.3	72.48	74.61	76.71	75.36
600	24.73	25.68	30.33	52.02	63.29	74.02	76.56	78.54	77.33
610	24.39	25.32	30.17	52.16	63.57	74.35	77.03	78.88	77.80
620	22.93	23.76	28.29	51.3	63.47	74.6	77.29	79.19	78.06
630	21.86	22.63	26.83	50.36	63.25	74.64	77.44	79.34	78.21
640	21.98	22.76	26.75	50.12	63.23	74.59	77.42	79.27	78.19
650	24.26	25.24	29.08	51.41	63.82	74.95	77.56	79.5	78.34
660	30.44	31.61	35.34	54.04	64.55	74.92	77.15	78.94	77.92
670	41.55	42.88	46.35	57.67	65.79	75.29	76.89	78.67	77.66
680	56.44	57.39	59.65	61.88	67.82	76.1	76.9	78.67	77.67
690	66.74	67.34	68.95	65.34	69.73	76.61	76.85	78.5	77.62
700	72.49	72.86	73.72	66.86	70.32	76.32	76.25	77.99	77.01

Table 10. Spectral reflectance data of the fiber composite (# 8) prepared at 3:1 PEO: PCDA, 1.33 w/w % concentration, and 0.2 ml hr<sup>-1</sup> injection speed.

Wavelength (nm)	Treatment Temperature								
	25 °C	50 °C	60 °C	70 °C	80 °C	90 °C	100 °C	110 °C	120 °C
400	41.98	40.71	38.66	35.82	38.08	43.67	43.58	45.32	47.13
410	40.91	39.72	37.06	34.02	36.45	42.1	42.2	43.64	45.39
420	39.24	38.18	35.41	32.22	34.32	39.82	40	41.82	43.49
430	37.98	36.99	33.93	30.43	32.26	37.61	37.93	39.73	41.32
440	36.69	35.81	32.09	28.24	30.11	35.61	36.07	37.75	39.26
450	35.28	34.5	30.66	26.77	28.44	33.81	34.37	36.1	37.54
460	33.91	33.22	29.2	25.49	27.06	32.48	33.13	34.82	36.21
470	32.69	32.11	27.88	24.42	25.91	31.35	32.09	33.65	35.00
480	31.46	31.07	26.21	23.07	24.78	30.57	31.47	32.67	33.98
490	29.56	29.31	25.15	22.56	23.89	29.43	30.31	32.02	33.30
500	28.14	28.08	24.14	22.17	23.59	29.23	30.14	31.59	32.85
510	26.62	26.83	23.31	22.24	23.79	29.63	30.57	32.09	33.37
520	25.33	25.74	22.51	22.43	24.12	30.22	31.23	33.12	34.44
530	23.86	24.35	21.56	22.16	23.73	29.79	30.86	33.56	34.90
540	22.66	23.27	20.89	21.9	23.37	29.36	30.45	33.02	34.34
550	21.55	22.31	20.87	22.78	24.25	30.18	31.11	33.02	34.34
560	20.87	21.8	21.03	26.08	28.04	34.82	35.28	37.49	38.99
570	20.23	21.16	20.89	31.18	33.54	43.91	47.21	51.42	53.48
580	19.79	20.72	20.71	33.89	36.48	49.48	55.91	62.93	65.45
590	19.74	20.69	20.64	34.94	37.69	52.25	61.18	70.99	73.83
600	19.9	20.86	20.85	35.53	38.27	53.4	63.52	74.6	77.58
610	19.62	20.54	20.73	35.74	38.4	53.74	64.38	75.56	78.58
620	18.71	19.62	19.7	35	37.74	53.64	64.77	76.09	79.13
630	18.1	18.94	19.06	34.32	37.01	53.3	65.08	76.48	79.54
640	18.29	19.15	19.27	34.34	37	53.29	65.46	76.55	79.61
650	19.57	20.38	20.49	35.42	38.08	54.16	66.38	76.95	80.03
660	23.91	24.56	24.61	37.94	40.46	55.81	67.29	76.46	79.52
670	31.9	32.17	32.07	42.56	45.09	59.21	68.63	76.28	79.33
680	44.44	43.41	43.92	50.38	53.01	64.69	70.08	76.31	79.36
690	55.74	53.2	55.79	58.69	61.58	69.59	70.74	76.25	79.30
700	62.64	58.76	62.81	63.42	66.23	71.68	70.56	75.8	78.83

Table 11. Spectral reflectance data of the fiber composite (# 9) prepared at 3:1 PEO: PCDA, 3.34 w/w % concentration, and 0.1 ml hr<sup>-1</sup> injection speed.

Wavelength (nm)	Treatment Temperature								
	25 °C	50 °C	60 °C	70 °C	80 °C	90 °C	100 °C	110 °C	120 °C
400	28	25.12	22.75	20.34	21.04	22.89	23.21	26.19	26.53
410	26.65	23.66	21.19	18.97	19.74	21.34	21.5	24.43	24.75
420	25.09	22.26	19.53	17.32	18.08	19.4	19.56	22.33	22.62
430	23.75	21.03	17.97	15.88	16.65	17.68	17.79	20.26	20.52
440	22.51	19.77	16.61	14.78	15.51	16.44	16.48	18.67	18.91
450	21.29	18.75	15.51	13.97	14.67	15.5	15.56	17.44	17.67
460	20.14	17.74	14.62	13.4	14.08	14.92	14.99	16.65	16.87
470	19.09	16.86	13.84	13.02	13.73	14.54	14.64	16.12	16.33
480	18.01	15.86	13.15	12.72	13.48	14.39	14.46	15.89	16.10
490	16.86	15.14	12.67	12.57	13.26	14.2	14.41	15.72	15.92
500	15.84	14.4	12.45	12.68	13.42	14.42	14.66	15.96	16.17
510	14.89	13.67	12.46	12.88	13.63	14.66	14.94	16.52	16.73
520	14.07	13.02	12.45	13.03	13.82	14.84	15.09	17.06	17.28
530	13.31	12.44	12.13	12.91	13.69	14.71	14.97	17.07	17.29
540	12.76	12.05	11.94	13.03	13.81	14.91	15.23	16.96	17.18
550	12.32	11.79	12.34	13.62	14.41	15.51	15.81	17.55	17.78
560	12.01	11.55	13.28	16.86	17.39	19.53	20.18	23.48	23.79
570	11.76	11.33	13.51	25.84	26.12	31.41	34.28	39.54	40.05
580	11.68	11.28	13.61	33.28	33.27	43	50.14	56.12	56.85
590	11.73	11.33	13.71	37.68	37.41	50.68	61.79	67.68	68.56
600	11.85	11.46	13.97	39.68	39.31	54.13	66.99	72.85	73.80
610	11.77	11.39	13.88	40.23	39.92	55.25	68.49	74.28	75.25
620	11.49	11.05	13.26	39.58	39.27	55.52	69.06	74.9	75.87
630	11.5	11.07	12.99	38.71	38.38	55.57	69.53	75.36	76.34
640	11.82	11.41	13.34	38.83	38.32	55.9	69.77	75.51	76.49
650	12.51	12.19	14.68	40.78	39.88	57.14	70.19	75.85	76.84
660	16.04	15.75	19.02	44.98	43.57	59.02	69.86	75.41	76.39
670	24.8	23.96	28.01	51.38	49.38	62.02	69.8	75.2	76.18
680	39.64	37.49	42.55	59.33	57.07	65.83	70.02	75.28	76.26
690	56.11	52.46	58.28	65.58	63.65	68.68	70.11	75.23	76.21
700	66.78	61.66	67.91	68.41	66.79	69.63	69.67	74.69	75.66

Table 12. Spectral reflectance data of the fiber composite (# 10) prepared at 3:1 PEO: PCDA, 3.34 w/w % concentration, and 0.2 ml hr<sup>-1</sup> injection speed.

Wavelength (nm)	Treatment Temperature								
	25 °C	50 °C	60 °C	70 °C	80 °C	90 °C	100 °C	110 °C	120 °C
400	29.5	28.26	23.88	22.29	22.95	23.64	25.49	22.71	20.44
410	28.27	27.01	22.73	20.85	21.7	22.21	23.5	21.39	19.25
420	26.46	25.08	20.78	19.22	20.05	20.45	21.62	19.91	17.92
430	24.97	23.45	19.07	17.83	18.66	18.98	19.94	18.58	16.72
440	23.77	22.09	17.78	16.52	17.52	17.77	18.24	17.61	15.85
450	22.38	20.65	16.53	15.67	16.67	16.88	17.29	16.85	15.17
460	21.13	19.4	15.6	15.04	16.08	16.28	16.57	16.41	14.77
470	19.98	18.29	14.85	14.63	15.71	15.93	16.12	16.12	14.51
480	19.02	17.4	14.42	14.25	15.54	15.78	15.58	16.11	14.50
490	17.55	16.14	13.63	14.03	15.2	15.45	15.6	15.96	14.36
500	16.51	15.41	13.58	14.12	15.39	15.67	15.74	16.13	14.52
510	15.53	14.74	13.78	14.28	15.68	15.94	15.9	16.47	14.82
520	14.68	14.13	13.99	14.43	15.91	16.17	16.01	16.72	15.05
530	13.8	13.34	13.57	14.28	15.73	15.97	15.98	16.68	15.01
540	13.12	12.85	13.3	14.36	15.84	16.09	16.2	16.81	15.13
550	12.59	12.57	13.8	14.7	16.24	16.41	16.58	17.11	15.40
560	12.31	12.42	15.86	17.7	19.03	19.72	20.74	19.8	17.82
570	11.96	12.08	17.96	28.05	29.73	32.59	35.71	31.92	28.73
580	11.82	11.95	18.99	38.4	41.27	48.02	52.94	46.29	41.66
590	11.85	11.98	19.51	45.49	49.86	60.18	65.22	57.26	51.53
600	11.98	12.13	20.06	49.02	54.17	65.93	70.54	62.26	56.03
610	11.93	12.05	19.84	50.04	55.69	67.69	72.01	63.73	57.36
620	11.57	11.63	18.39	49.46	55.95	68.25	72.43	64.07	57.66
630	11.44	11.48	17.19	49.03	56.37	68.74	72.79	64.45	58.01
640	11.6	11.65	17.17	50.37	57.58	68.95	72.86	64.51	58.06
650	11.92	12.16	19.97	54.47	60.04	69.32	73.06	64.8	58.32
660	15.23	15.84	26.98	60.29	62.52	68.96	72.6	64.4	57.96
670	24.94	26.11	40.32	65.43	64.49	68.76	72.28	64.24	57.82
680	42.57	44.32	56.5	68.74	65.81	68.81	72.25	64.28	57.85
690	59.33	60.7	63.81	69.9	66.31	68.78	72.23	64.2	57.78
700	68.86	69.77	66.84	69.98	66.23	68.34	71.81	63.8	57.42

Table 13. Spectral reflectance data of the fiber composite (# 11) prepared at 3:1 PEO: PCDA, 6.67 w/w % concentration, and 0.1 ml hr<sup>-1</sup> injection speed.

Wavelength (nm)	Treatment Temperature								
	25 °C	50 °C	60 °C	70 °C	80 °C	90 °C	100 °C	110 °C	120 °C
400	34.93	34.12	33.13	26.95	26.83	29.36	31.9	33.07	34.39
410	33.58	32.64	31.56	25.32	25.23	27.24	29.58	31.13	32.38
420	31.56	30.38	28.99	22.97	22.97	25.03	27.03	28.35	29.48
430	29.81	28.39	26.61	20.75	20.9	22.83	24.52	25.6	26.62
440	28.34	26.8	24.76	19.09	19.2	20.73	22.2	23.44	24.38
450	26.61	25.04	22.82	17.65	17.83	19.31	20.57	21.52	22.38
460	25.04	23.5	21.29	16.65	16.85	18.24	19.4	20.25	21.06
470	23.58	22.13	19.92	15.84	16.1	17.4	18.48	19.24	20.01
480	22.24	21.06	19.13	15.39	15.61	16.59	17.72	18.8	19.55
490	20.34	19.42	17.7	14.73	15.07	16.29	17.35	18.1	18.82
500	18.87	18.4	17.36	14.79	15.13	16.27	17.36	18.18	18.91
510	17.46	17.46	17.48	15.17	15.47	16.53	17.69	18.83	19.58
520	16.28	16.57	17.55	15.56	15.84	16.81	18.09	19.71	20.50
530	15.09	15.52	16.75	15.23	15.56	16.67	17.95	19.71	20.50
540	14.13	14.73	16.18	14.99	15.39	16.55	17.82	19.24	20.01
550	13.36	14.18	16.7	15.68	16.07	17.2	18.39	19.58	20.36
560	12.92	13.9	18.46	21.48	21.59	24.03	26.23	27.79	28.90
570	12.5	13.43	18.59	34.03	34.13	39.54	44.37	46.13	47.98
580	12.31	13.19	18.49	44.14	44.25	52.47	60.32	61.72	64.19
590	12.3	13.21	18.59	49.94	49.84	59.47	69.1	70.18	72.99
600	12.44	13.4	18.97	52.5	52.25	62.31	72.3	73.26	76.19
610	12.33	13.25	18.69	53.21	53.03	63.23	73.09	73.99	76.95
620	11.85	12.61	17.41	52.85	52.65	63.38	73.41	74.31	77.28
630	11.69	12.31	16.41	52.29	52.2	63.53	73.65	74.54	77.52
640	11.89	12.49	16.43	52.74	52.51	63.89	73.67	74.55	77.53
650	12.62	13.77	18.81	55.2	54.35	64.94	73.88	74.78	77.77
660	16.87	18.95	25.27	59.23	57.38	65.93	73.47	74.3	77.27
670	28.38	31.2	37.55	63.78	60.57	67.1	73.23	74.04	77.00
680	48	50.87	55.78	67.56	63.26	68.29	73.29	74.09	77.05
690	64.17	65.93	67.57	69.38	64.68	68.91	73.23	73.95	76.91
700	72.74	74.15	73.25	69.94	64.98	68.91	72.73	73.48	76.42

Table 14. Spectral reflectance data of the fiber composite (# 12) prepared at 3:1 PEO: PCDA, 6.67 w/w % concentration, and 0.2 ml hr<sup>-1</sup> injection speed.

Wavelength (nm)	Treatment Temperature								
	25 °C	50 °C	60 °C	70 °C	80 °C	90 °C	100 °C	110 °C	120 °C
400	29.91	30.84	24.52	30.86	32.03	33.07	34.18	33.53	32.89
410	28.81	29.82	23.23	29.89	30.87	31.89	32.93	32.34	31.73
420	27.34	28.06	21.63	28.13	29.37	30.47	31.4	30.75	30.17
430	26.16	26.67	20.2	26.63	28.12	29.21	30.08	29.19	28.64
440	25	25.5	18.85	25.5	26.9	27.98	28.87	28.09	27.56
450	23.77	24.14	17.79	24.45	25.99	27.09	27.91	27.05	26.54
460	22.6	22.93	16.91	23.72	25.33	26.44	27.23	26.39	25.89
470	21.57	21.89	16.2	23.19	24.87	26	26.75	25.9	25.41
480	20.51	21.02	15.53	23	24.45	25.52	26.39	25.74	25.25
490	19.17	19.59	14.99	22.3	24.06	25.18	25.97	25.31	24.83
500	18.06	18.7	14.8	22.36	24.06	25.15	25.94	25.37	24.89
510	16.97	17.78	14.85	22.63	24.21	25.29	26.16	25.79	25.30
520	16.05	17.01	14.94	22.98	24.43	25.53	26.44	26.31	25.81
530	15.12	16.1	14.64	22.64	24.21	25.33	26.25	26.32	25.82
540	14.43	15.43	14.4	22.42	24.11	25.24	26.15	26.36	25.86
550	13.85	14.89	14.78	22.65	24.39	25.49	26.31	26.61	26.10
560	13.45	14.61	16.42	25.4	26.94	28.06	28.96	29.38	28.82
570	13.11	14.2	17.83	36.01	38.01	39.81	41.48	42.06	41.26
580	12.94	13.99	18.39	45.87	48.42	51.53	54.79	55.34	54.29
590	12.9	13.97	18.56	53.07	55.89	60.33	65.46	66.09	64.83
600	13.02	14.11	18.99	56.58	59.47	64.52	70.53	71.26	69.91
610	13.04	14.09	19.03	57.65	60.57	65.85	71.98	72.64	71.26
620	12.64	13.61	17.87	57.45	60.44	66.26	72.54	73.21	71.82
630	12.46	13.34	16.88	57.06	60.17	66.61	72.94	73.59	72.19
640	12.6	13.43	16.65	57.64	60.65	67.04	73.16	73.66	72.26
650	12.46	13.54	17.9	60.16	62.61	67.76	73.53	74.06	72.65
660	14.77	16.43	22.78	63.75	65.27	68.2	73.22	73.56	72.16
670	22.25	24.93	33.63	67.8	68.2	68.86	73.1	73.37	71.98
680	36.79	40.72	51.32	71.46	70.95	69.93	73.35	73.46	72.06
690	53.33	56.68	63.09	73.55	72.55	70.71	73.43	73.5	72.10
700	63.6	66.2	69.09	74.21	73.23	70.82	73.1	72.84	71.46

**Appendix 4: Reflectance values for fiber composites prepared at 4:1 PEO: PCDA**

Table 15. Spectral reflectance data of the fiber composite (# 13) prepared at 4:1 PEO: PCDA, 1.25 w/w % concentration, and 0.1 ml hr<sup>-1</sup> injection speed.

Wavelength (nm)	Treatment Temperature								
	25 °C	50 °C	60 °C	70 °C	80 °C	90 °C	100 °C	110 °C	120 °C
400	35.02	32.76	29.31	33.1	32.29	37.36	37.37	36.94	31.09
410	33.63	31.21	27.66	31.28	30.16	35.24	35.25	35.09	29.13
420	31.89	29.51	26.14	28.67	27.58	32.33	32.7	32.27	26.84
430	30.38	27.88	24.52	25.97	24.84	29.25	29.82	29.5	24.53
440	29.05	26.42	22.95	23.72	22.49	26.5	27.13	27.13	22.26
450	27.56	24.92	21.59	21.74	20.6	24.25	25.03	25.02	20.61
460	26.22	23.58	20.38	20.36	19.3	22.68	23.48	23.55	19.43
470	24.96	22.31	19.21	19.17	18.19	21.33	22.08	22.3	18.44
480	23.71	21.09	18.02	18.42	17.44	20.27	20.86	21.51	17.6
490	22.19	19.89	17.18	17.51	16.77	19.46	20.19	20.46	17.18
500	20.89	18.84	16.43	17.34	16.64	19.25	19.85	20.28	17.03
510	19.55	17.82	15.93	17.6	16.85	19.44	20	20.63	17.2
520	18.38	16.87	15.43	17.94	17.08	19.8	20.37	21.24	17.52
530	17.28	16.03	14.79	17.58	16.83	19.55	20.21	20.95	17.42
540	16.45	15.53	14.34	17.36	16.74	19.29	19.84	20.48	17.24
550	15.73	15.19	14.37	18	17.24	19.79	20.17	20.73	17.53
560	15.17	14.85	14.64	21.58	21.4	25.86	26.03	26.21	22.04
570	14.7	14.44	14.51	31.25	33.1	42.25	42.08	41.84	36.37
580	14.41	14.18	14.36	38.23	43.05	58.15	57.49	57.67	51.64
590	14.31	14.11	14.29	41.85	48.75	68.08	67.02	68.19	61.89
600	14.46	14.27	14.49	43.71	51.32	72.13	70.75	72.45	66.2
610	14.48	14.34	14.58	44.45	52.15	73.35	71.86	73.55	67.57
620	13.91	13.74	13.9	42.71	51.05	73.81	72.19	74.05	67.84
630	13.57	13.37	13.46	40.19	49.43	74.29	72.57	74.43	68.3
640	13.75	13.54	13.6	38.82	48.83	74.58	72.64	74.47	68.47
650	14.2	14	14.17	40.48	50.78	75	72.88	74.55	68.66
660	16.98	16.75	17.12	45.93	55.35	74.83	72.49	73.96	68.35
670	23.98	23.72	24.46	55.26	61.95	74.58	72.17	73.83	68.08
680	37.44	37.31	38.61	64.53	67.82	74.66	72.2	74.35	68.14
690	54.26	54.13	53.93	68.73	70.35	74.88	72.19	74.6	68.23
700	64.42	64.12	62.2	70.16	71	74.72	71.89	74.48	67.75

Table 16. Spectral reflectance data of the fiber composite (# 14) prepared at 4:1 PEO: PCDA, 1.25 w/w % concentration, and 0.2 ml hr<sup>-1</sup> injection speed.

Wavelength (nm)	Treatment Temperature								
	25 °C	50 °C	60 °C	70 °C	80 °C	90 °C	100 °C	110 °C	120 °C
400	34.34	37.38	44.45	30.89	40.43	36.17	38.77	41.51	38.24
410	33.31	36.46	43.7	29.21	39.37	35.23	37.85	40.49	37.3
420	31.64	34.74	41.59	27.52	36.87	33.01	35.51	38.13	35.14
430	30.25	33.14	39.64	25.7	34.37	30.79	33.17	35.94	33.09
440	29.08	32.04	38.45	23.85	32.56	29.16	31.53	34.29	31.52
450	27.67	30.45	36.46	22.4	30.34	27.4	29.67	32.43	29.84
460	26.41	29.13	34.85	21.25	28.79	26.26	28.48	31.19	28.74
470	25.27	27.86	33.3	20.2	27.34	25.26	27.42	30.12	27.77
480	24.24	27.02	32.53	19.16	26.64	24.78	27	29.68	27.28
490	22.61	25.1	30.05	18.56	24.85	23.65	25.69	28.22	26.14
500	21.43	23.92	28.9	18.18	24.5	23.53	25.57	27.98	25.95
510	20.27	22.87	28.02	18.24	24.89	23.89	26	28.42	26.35
520	19.29	21.96	27.25	18.41	25.47	24.45	26.68	29.29	27.08
530	18.21	20.74	25.75	18.2	24.81	24.11	26.31	29	26.86
540	17.37	19.79	24.59	18.01	24.13	23.79	25.86	28.33	26.33
550	16.65	19.01	23.88	18.57	24.64	24.38	26.31	28.34	26.46
560	16.2	18.66	24	20.77	28.11	27.85	30.25	31.96	29.79
570	15.72	18.13	23.4	23.86	31.88	36.7	42.58	44.46	41.8
580	15.46	17.77	22.94	25.47	33.79	43.03	54.04	56.5	53.84
590	15.43	17.77	22.98	26.13	34.76	46.94	63.15	66.45	64.08
600	15.55	17.93	23.16	26.5	35.18	48.8	67.83	71.44	69.39
610	15.41	17.7	22.83	26.64	35.04	49.48	69.56	72.88	71.07
620	14.84	17	21.97	26.11	34.65	49.6	70.4	73.48	71.58
630	14.55	16.54	21.26	25.6	33.96	49.5	71.19	73.93	72.06
640	14.85	16.78	21.46	25.54	33.88	49.69	71.8	74.07	72.32
650	15.64	17.73	22.63	26.28	34.83	50.81	72.6	74.24	72.59
660	18.44	20.76	26.06	28.07	36.79	53	72.8	73.73	72.2
670	24.22	26.84	32.89	32.03	40.97	57.01	73.14	73.64	71.96
680	33.66	36.83	44.04	40.23	48.81	63.29	73.51	73.97	71.97
690	47.13	48.87	55.63	52.64	58.89	68.38	73.56	74.04	71.89
700	57.39	57.68	63.48	61.49	65.66	70.76	73.32	73.82	71.51

Table 17. Spectral reflectance data of the fiber composite (# 15) prepared at 4:1 PEO: PCDA, 3.13 w/w % concentration, and 0.1 ml hr<sup>-1</sup> injection speed.

Wavelength (nm)	Treatment Temperature								
	25 °C	50 °C	60 °C	70 °C	80 °C	90 °C	100 °C	110 °C	120 °C
400	35.39	36.38	33.48	27.76	28.67	27.33	28.42	30.97	35.29
410	34.1	35.04	31.77	26.19	27.14	26.03	26.6	28.83	32.97
420	32.35	33.08	29.8	24.06	24.9	24.45	24.5	26.62	31.02
430	30.86	31.2	27.66	21.83	22.64	22.87	22.29	24.44	28.98
440	29.43	29.73	25.83	20.07	20.85	21.12	20.28	22.24	26.53
450	27.89	28	24.1	18.5	19.24	19.9	18.85	20.78	25.13
460	26.5	26.54	22.68	17.39	18.13	18.96	17.85	19.7	24.02
470	25.2	25.13	21.27	16.4	17.16	18.17	17.1	18.88	23.14
480	23.79	24.02	20.13	15.78	16.57	17.32	16.49	18.12	21.9
490	22.09	22.28	19	15.09	15.84	17.08	16.28	17.92	22.01
500	20.62	21.04	18.37	14.98	15.77	16.96	16.41	17.94	21.89
510	19.17	19.92	18.24	15.34	16.14	17.16	16.76	18.28	22.07
520	17.93	18.88	18.04	15.75	16.56	17.49	17.1	18.7	22.41
530	16.75	17.7	17.33	15.47	16.27	17.45	17.06	18.74	22.64
540	15.77	16.75	16.75	15.24	16.03	17.34	17.14	18.69	22.59
550	14.91	16.01	17.01	16.14	16.88	17.98	17.84	19.22	23.14
560	14.3	15.54	18.02	19.98	20.75	22.11	23.14	24.58	28.44
570	13.85	15.03	18.07	27.2	29.22	33.78	38.44	40.26	44.34
580	13.61	14.72	17.94	31.51	34.53	44.26	54.43	56.38	59.32
590	13.6	14.74	17.96	33.53	37.13	50.69	65.16	66.85	68.33
600	13.82	15.01	18.33	34.46	38.27	53.38	69.58	71.11	71.97
610	13.79	14.92	18.32	34.73	38.54	54.41	70.78	72.22	73.02
620	13.14	14.07	17.18	33.81	37.74	54.44	71.12	72.64	73.3
630	12.84	13.58	16.28	32.31	36.39	54.75	71.49	72.96	73.64
640	13.11	13.85	16.3	31.48	35.69	54.84	71.57	72.95	73.78
650	14.01	15.12	17.59	32.43	36.78	54.99	71.8	72.97	73.93
660	17.62	19.28	21.72	36.23	40.48	54.75	71.33	72.42	73.5
670	25.71	27.85	29.94	43.54	47.12	54.47	70.98	72.36	73.2
680	39.29	41.69	43.34	55.14	56.76	54.46	70.93	72.77	73.22
690	57.31	58.66	59.95	65.65	64.53	54.57	70.83	73.02	73.14
700	69.24	69.3	70.31	70.68	68.15	54.15	70.38	72.74	72.7

Table 18. Spectral reflectance data of the fiber composite (# 16) prepared at 4:1 PEO: PCDA, 3.13 w/w % concentration, and 0.2 ml hr<sup>-1</sup> injection speed.

Wavelength (nm)	Treatment Temperature								
	25 °C	50 °C	60 °C	70 °C	80 °C	90 °C	100 °C	110 °C	120 °C
400	37.32	40.13	46.66	37.48	36.26	35.25	39.88	36	39.33
410	36.05	39.09	46.19	36.34	34.64	33.67	39.22	34.64	38.03
420	34.35	37.14	43.65	33.8	32.08	31.22	36.91	32.32	35.24
430	32.93	35.37	41.46	31.3	29.51	28.79	34.8	30.24	32.7
440	31.55	34.14	40.25	29.54	27.45	26.64	33.32	28.44	30.72
450	30.1	32.41	38.07	27.56	25.58	24.87	31.48	26.81	28.71
460	28.7	30.93	36.42	26.25	24.31	23.65	30.3	25.68	27.4
470	27.41	29.53	34.95	25.12	23.27	22.66	29.36	24.83	26.34
480	26.04	28.66	34.75	24.84	22.74	21.95	29.44	24.43	26.05
490	24.47	26.56	31.84	23.33	21.8	21.23	27.76	23.47	24.71
500	23.07	25.36	31.34	23.32	21.79	21.25	27.93	23.48	24.83
510	21.6	24.29	31.25	23.84	22.18	21.61	28.56	23.91	25.44
520	20.34	23.33	31.26	24.46	22.64	22.11	29.42	24.56	26.3
530	19.15	21.98	29.72	23.86	22.25	21.88	28.92	24.29	25.92
540	18.25	20.97	28.63	23.42	22.03	21.74	28.4	23.94	25.42
550	17.43	20.16	28.24	23.93	22.52	22.3	28.49	24.12	25.63
560	16.83	19.93	29.33	27.43	26.93	27.18	31.81	27.88	30.46
570	16.39	19.36	28.72	34.46	40.13	42.11	44.19	41.18	45.38
580	16.1	18.96	28.22	38.87	52.11	56.9	55.27	54.21	59.62
590	16.01	18.98	28.37	41.28	60.09	66.8	62.67	63	68.96
600	16.21	19.18	28.6	42.63	63.78	71.07	65.76	66.73	72.81
610	16.23	19.02	28.13	42.82	65.02	72.38	66.78	67.87	73.89
620	15.56	18.34	27.38	41.24	65.52	72.84	66.94	68.14	74.24
630	15.17	17.84	26.51	39.1	66.01	73.3	67.23	68.49	74.58
640	15.24	17.88	26.43	38.44	66.93	73.47	67.24	68.5	74.71
650	15.38	18.17	26.99	40.88	68.65	73.81	67.42	68.48	74.88
660	18.48	21.55	30.74	47.4	69.98	73.52	67.06	68.06	74.48
670	27.51	30.91	40.16	57.45	71.19	73.34	66.74	67.96	74.19
680	44.57	48.18	56.84	66.63	72.36	73.46	66.77	68.24	74.21
690	61.57	63.78	69.61	70.65	72.87	73.47	66.68	68.52	74.04
700	70.9	72.13	76.02	72.33	72.79	73.36	66.43	68.23	73.76

Table 19. Spectral reflectance data of the fiber composite (# 17) prepared at 4:1 PEO: PCDA, 6.25 w/w % concentration, and 0.1 ml hr<sup>-1</sup> injection speed.

Wavelength (nm)	Treatment Temperature								
	25 °C	50 °C	60 °C	70 °C	80 °C	90 °C	100 °C	110 °C	120 °C
400	27.34	26.56	24.18	23.11	23.49	22.21	23.07	25.79	26.5
410	26.19	25.2	22.78	21.76	22.18	21.1	21.97	24.43	25.32
420	24.65	23.67	21.22	20.2	20.42	19.71	20.41	22.59	23.48
430	23.35	22.2	19.67	18.57	18.72	18.4	18.94	20.97	21.84
440	22.19	21.02	18.46	17.31	17.41	17.21	17.67	19.56	20.58
450	20.97	19.76	17.27	16.2	16.24	16.37	16.75	18.46	19.47
460	19.83	18.69	16.3	15.44	15.44	15.78	16.1	17.71	18.77
470	18.8	17.68	15.37	14.76	14.8	15.33	15.65	17.17	18.28
480	17.72	16.81	14.64	14.34	14.43	14.83	15.2	16.82	18.13
490	16.54	15.84	13.93	13.91	13.94	14.77	15.11	16.46	17.7
500	15.52	15.03	13.47	13.85	13.96	14.81	15.24	16.61	17.92
510	14.52	14.26	13.17	14.12	14.23	14.94	15.48	16.96	18.29
520	13.7	13.57	12.86	14.39	14.53	15.11	15.73	17.37	18.69
530	12.95	12.92	12.39	14.21	14.32	15.07	15.67	17.23	18.47
540	12.41	12.48	12.11	14.14	14.23	15.18	15.78	17.18	18.42
550	11.97	12.15	12.17	14.85	14.89	15.88	16.53	17.77	19.03
560	11.67	11.93	12.36	17.5	17.61	19.03	20.21	21.6	22.74
570	11.43	11.64	12.17	22.82	24.63	29.2	32.67	34.46	35.72
580	11.36	11.54	12.09	26.02	29.35	39.56	47.93	49.6	51.1
590	11.38	11.58	12.11	27.41	31.7	47.32	61.24	61.67	63.76
600	11.49	11.72	12.28	28.09	32.74	51.26	67.98	67.16	69.69
610	11.49	11.73	12.31	28.39	33.05	52.8	70.04	68.54	71.27
620	11.25	11.41	11.9	27.33	31.98	52.84	70.55	68.99	71.68
630	11.31	11.4	11.78	25.67	30.29	52.57	71.09	69.32	72.07
640	11.69	11.76	12.09	24.58	29.2	52.49	71.3	69.15	72.19
650	12.01	12.13	12.54	24.98	29.71	53.52	71.53	68.76	72.39
660	13.77	14.13	14.54	27.66	32.62	56.25	70.99	67.86	71.83
670	19.13	19.76	19.99	34.09	39.21	60.65	70.62	67.84	71.52
680	30.14	31.02	30.79	45.52	50.95	66.08	70.56	68.91	71.43
690	46.85	48.07	47.36	59.21	63.06	69.74	70.55	69.89	71.34
700	60.55	61.52	61.21	66.86	69.37	70.98	70.31	70.06	70.8

Table 20. Spectral reflectance data of the fiber composite (# 18) prepared at 4:1 PEO: PCDA, 6.25 w/w % concentration, and 0.2 ml hr<sup>-1</sup> injection speed.

Wavelength (nm)	Treatment Temperature								
	25 °C	50 °C	60 °C	70 °C	80 °C	90 °C	100 °C	110 °C	120 °C
400	32.93	35.12	28.49	29.21	27.62	46.12	27.74	34.12	29.22
410	31.2	35.13	27.96	28.71	26.17	46.98	26.74	34.14	28.17
420	30.67	32.88	25.94	26.65	25.2	44.33	25.82	32.39	27.48
430	30.28	31.29	24.29	24.97	24.27	42.58	24.98	31.37	26.86
440	28.9	30.76	23.34	24.1	22.92	42.37	23.92	30.97	25.93
450	28.53	29.08	21.82	22.79	22.33	40.61	23.38	29.98	25.56
460	27.8	27.89	20.77	22.01	21.82	39.76	22.99	29.43	25.28
470	27.21	26.95	19.86	21.48	21.5	39.32	22.75	29.25	25.15
480	25.33	27.28	19.75	21.81	20.66	40.88	22.22	29.88	24.61
490	25.68	24.59	18.11	20.49	21.01	37.84	22.47	28.39	25
500	24.58	24.2	17.92	20.73	20.91	38.56	22.51	28.78	25.01
510	23.15	23.97	18	21.2	20.77	39.58	22.49	29.31	24.96
520	21.85	23.99	18.2	21.78	20.66	40.9	22.47	30.02	24.88
530	21.46	22.73	17.47	21.27	20.72	39.8	22.5	29.42	24.94
540	21.36	21.83	16.95	21.02	20.99	39.15	22.8	29.07	25.19
550	21.15	21.18	16.89	21.26	21.48	39	23.25	29.04	25.61
560	20.06	21.8	17.76	23.03	22.1	41.11	23.86	30	25.69
570	20.1	21.19	17.63	28.16	28.28	48.18	33.21	36.27	34.47
580	20.07	20.85	17.5	32.51	33.54	56.26	45.99	44.02	46.03
590	19.86	21.04	17.61	35.87	37.18	64.87	60.5	52.73	59.17
600	20	21.07	17.72	37.64	39.23	69.89	70.1	58.15	67.83
610	20.32	20.63	17.55	38.14	40.14	71.66	73.69	60.15	71.03
620	19.73	20.61	17.21	37.63	39.33	72.46	74.59	60.48	71.65
630	19.62	20.39	16.85	36.49	38.3	73.04	75.47	60.87	72.32
640	19.75	20.57	16.92	36.03	37.97	73.43	75.87	60.79	72.62
650	19.78	20.94	17.3	37.3	39.16	74.12	76.17	60.5	72.81
660	20.38	21.28	18.23	40.94	43.11	74.11	75.68	59.88	72.38
670	24.7	25.67	23.06	48.21	50.29	74.29	75.24	59.91	72.11
680	34.12	35.28	33.64	59.49	60.95	74.87	75.23	60.86	72.1
690	48.67	50.06	49.97	69.44	69.78	75.33	75.4	61.78	72.05
700	59.97	61.89	62.98	74.41	74.29	75.11	75.13	61.75	71.57